On the impact of aromatic core fluorination in hydrogen-bonded liquid crystals

Ahmed F. Darweesh,*[a] Christian Anders,[b] B. S. Ranjitha,[c] G. Shanker,[c] Mohamed Alaasar*[a,b]

[a]Department of Chemistry, Faculty of Science, Cairo University, 12613 Giza, Egypt
[b]Institute of Chemistry, Martin Luther University Halle-Wittenberg, 06120 Halle, Germany
[c]Department of Chemistry, Bangalore University, Jnana Bharathi Campus, Bengaluru, 560056, India

Contents

1. Experimental

1.1. Characterization

Chemicals of analytical purity, sourced from commercial suppliers, were utilized as received. Solvents, when required, underwent drying using conventional techniques. Various spectral data were employed to confirm the purity and chemical composition of all synthesized compounds. Structure characterization of the produced materials was assessed by utilizing ^{1}H NMR, ^{13}C NMR, and ^{19}F NMR with Varian Unity 400 spectrometers in $CDCl_3$ solution. ^{1}H NMR and ^{13}C NMR chemical shifts are reported in ppm referenced to tetramethylsilane. The residual proton signal of the deuterated solvent was used as internal standard for ^{1}H NMR and ^{13}C NMR spectra. ^{19}F NMR chemical shifts are reported in ppm refernced to trichlorofluoromethane as an external standard.

Infrared absorption spectra were measured in dry KBr with a Perkin-Elmer B25 spectrophotometer.

The assessment of mesophase phases and the determination of transition temperatures for the hydrogen-bonded compounds involved using a Nikon Optiphot-2 polarizing microscope in conjunction with a Mettler FP-82 HT hot stage and control unit. Enthalpies were determined by analyzing DSC thermograms obtained with a Perkin-Elmer DSC-7 instrument, employing a heating and cooling rate of 10 K min^{-1}.

The photoisomerization studies in solution were conducted using Ocean Optics HR 2000+ spectrophotometer, and absorption spectra were recorded at room temperature. The solutions in chloroform were taken in a 1cm quartz cuvette and covered to avoid the evaporation of the solvent. The solutions were irradiated with UV light of 1mW/cm^2 using Bluepoint LED Eco Hönle at a wavelength of 365 nm. A heat filter is inserted between the sample and the source to avoid the influence of UV heat on the sample. The *trans-cis-trans* photoisomerization in the LC phase was performed using of 1 mW/cm^2 Bluepoint LED Eco Hönle at a wavelength of 365 nm.

X-ray investigations were carried out with an Incoatec (Geesthacht, Germany) IμS microfocus source with a monochromator for CuKα radiation (λ = 0.154 nm), calibration with the powder pattern of $Pb(NO_3)_2$. A droplet of the sample was placed on a glass plate on a Linkam hot stage HFS-X350-GI (rate: 1 K/min). Exposure time was 5 min; the sample-detector distance was 9.00 cm for WAXS and 26.80 cm for SAXS. The diffraction patterns were recorded with a Vantec 500 area detector (Bruker AXS, Karlsruhe) and transformed into 1D plots using GADDS software.

1.2. Synthesis

1.2.1. Synthesis of **B6F$_2$, B6F$_3$** *and* **B6F$_{23}$**

1.2.1.1. 2-Fluoro-4-n-hexyloxybenzoic acid, **B6F$_2$**

2-Fluoro-4-n-hexyloxybenzonitrile, **BF$_2$**

A suspension of 2-fluoro-4-hydroxybenzonitrile (2.74 g, 20 mmol, 1 eq.), 1-bromohexane (3.6 g, 22 mmol, 1.1 eq.), potassium carbonate (13.8 g, 100 mmol, 5 eq.) and a catalytic amount of *tetra-n*-butylammoniumiodide were refluxed in dry butanone for 5 hours. The solvent was

removed under vacuum and the crude product was purified by column chromatography (eluent: first hexane, then $CHCl_3$); yield 3.55 g (16 mmol, 80%); colourless liquid; $C_{13}H_{16}FNO$; *M* = 221.27 g/mol; ^{1}H NMR (400 MHz, $CDCl_3$) δ 7.49 (dd, *J* = 8.7 Hz, 7.5 Hz, 1H, Ar-H), 6.74 (dd, *J* = 8.7 Hz, 2.4 Hz, 1H, Ar-H), 6.69 (dd, *J* = 11.1 Hz, 2.3 Hz, 1H, Ar-H), 3.99 (t, *J* = 6.5 Hz, 2H, OCH_2CH_2), 1.84–1.75 (m, 2H, OCH_2CH_2), 1.49–1.40 (m, 2H, CH_2), 1.39–1.29 (m, 4H, CH_2), 0.91 (t, *J* = 7.0 Hz, 3H, CH_3); ^{19}F NMR (376 MHz, $CDCl_3$) δ –104.36 (dd, *J* = 11.0 Hz, 7.5 Hz).

2-Fluoro-4-n-hexyloxybenzoic acid, **B6F$_2$.**

A solution of 2-fluoro-4-*n*-hexyloxybenzonitrile (**BF$_2$)** (3.55 g, 16 mmol, 1 eq.) and potassium hydroxide (4.5 g, 80 mmol, 5 eq.) were refluxed in ethanol and water (2/1, v/v). Afterwards the solution is concentrated and acidified with concentrated hydrochloric acid and the resulting product was filtered off, washed with water and dried; yield 1.9 g (8 mmol, 50%); colourless solid; $C_{13}H_{17}FO_3$; *M* = 240.27 g/mol; Cr 110 ºC N 120 ºC Iso; ^{1}H NMR (400 MHz, $CDCl_3$) δ 7.96 (t, *J* = 8.7 Hz, 1H, Ar-H), 6.73 (dd, *J* = 8.9, 2.5 Hz, 1H, Ar-H), 6.64 (dd, *J* = 12.9, 2.4 Hz, 1H, Ar-H), 4.01 (t, *J* = 6.6 Hz, 2H, OCH_2CH_2), 1.87–1.73 (m, 2H, OCH_2CH_2), 1.48–1.44 (m, 2H, CH_2), 1.37–1.32 (m, 4H, CH_2), 0.91 (t, *J* = 7.0 Hz, 3H, CH_3); ^{13}C NMR (101 MHz, $CDCl_3$) δ 168.6, 165.4, 165.0, 162.8, 134.0, 110.7, 102.5, 68.7, 31.4, 28.8, 25.5, 22.5, 13.9; ^{19}F NMR (378 MHz, $CDCl_3$) δ –105.02 (dd, *J* = 12.8 Hz, 8.6 Hz).

1.2.1.2. 3-Fluoro-4-n-hexyloxybenzoic acid, **B6F$_3$**

3-Fluoro-4-n-hexyloxybenzaldehyde, **BF$_3$**

A suspension of 3-fluoro-4-hydroxybenzaldehyde (2.8 g, 20 mmol, 1 eq.), 1-bromohexane (3.6 g, 22 mmol, 1.1 eq.), potassium carbonate (13.8 g, 100 mmol, 5 eq.) and a catalytic amount of tetra-*n*-butylammoniumiodide were refluxed in dry butanone for 5 hours. The solvent was removed under vacuum and the crude product was purified by column chromatography (eluent: first hexane, then $CHCl_3$); yield 3.1 g (14 mmol, 70%); colourless liquid; $C_{13}H_{17}FO_2$; *M* = 224.27 g/mol; ^{1}H NMR (400 MHz, $CDCl_3$) δ 9.85 (s, 1H, CHO), 7.64–7.58 (m, 2H, Ar-H), 7.05 (t, *J* = 8.2 Hz, 1H, Ar-H), 4.11 (t, *J* = 6.6 Hz, 2H, OCH_2CH_2), 1.90–1.82 (m, 2H, OCH_2CH_2), 1.53–1.43 (m, 2H, CH_2), 1.40–1.30 (m, 4H, CH_2), 0.91 (t, *J* = 7.0 Hz, 3H, CH_3); ^{19}F NMR (376 MHz, $CDCl_3$) δ –132.96 (dd, *J* = 10.9 Hz, *J* = 7.1 Hz).

3-Fluoro-4-n-hexyloxybenzoic acid, **B6F$_3$**

A mixture of the 3-fluoro-4-*n*-hexyloxybenzaldehyde (**BF$_3$)** (3.1 g, 14 mmol, 1 eq.), resorcinol (1.9 g, 17.5 mmol, 1.25 eq.) were dissolved under stirring at room temperature in *tert*-butanol (140 mL). Afterwards a solution of $NaOCl_2$ (7.3 g, 81 mmol, 5.8 eq.) and $NaH_2PO_4.2H_2O$ (4.9 g, 42 mmol, 3 eq.) in distilled water (80 mL) were added dropwise. After finishing the reaction the solution was concentrated and acidified with concentrated hydrochloric acid and resulting product was filtered off, washed with water and dried; yield 2.0 g (8.4 mmol, 60%); colourless solid; $C_{13}H_{17}FO_3$; *M* = 240.27 g/mol; Cr 108 ^oC Iso; ^1H NMR (400 MHz, $CDCl_3$) δ 7.85 (ddd, *J* = 8.6, 1.9, 1.1 Hz, 1H, Ar-H), 7.78 (dd, *J* = 11.5, 2.0 Hz, 1H, Ar-H), 6.97 (t, *J* = 8.3 Hz, 1H, Ar-H), 4.08 (t, *J* = 6.6 Hz, 2H, OCH_2CH_2), 1.89–1.78 (m, 2H, OCH_2CH_2), 1.49–1.43 (m, 2H, CH_2), 1.36–1.31 (m, 4H, CH_2), 0.89 (t, *J* = 7.0 Hz, 3H, CH_3); ^{13}C NMR (101 MHz, $CDCl_3$) δ 170.6, 153.0, 152.1, 150.5, 127.4, 117.8, 113.3, 69.3, 31.4, 28.9, 25.4, 22.5, 13.9; ^{19}F NMR (378 MHz, $CDCl_3$) δ –133.86 (dd, *J* = 11.5 Hz, 8.1 Hz).

1.2.1.3. 2,3-Difluoro-4-n-hexyloxybenzoic acid, **B6F$_{23}$**

2,3-Difluoro-4-n-hexyloxybenzaldehyde, **BF$_{23}$**

Synthesized according to the procedure described above for **BF$_3$** from 2,3-difluoro-4-hydroxybenzbenzaldehyde (0.8 g, 5.0 mmol) and 1-bromohexane (0.91 g, 5.5 mmol); purification by column chromatography (eluent: first hexane, then $CHCl_3$); yield 1.0 g (4.1 mmol, 82%); colourless oil; $C_{13}H_{16}F_2O_2$; *M* = 242.26 g/mol; ^1H NMR (500 MHz, $CDCl_3$) δ 10.19 (s, 1H, CHO), 7.60 (ddd, *J* = 9.1 Hz, 7.2 Hz, 2.2 Hz, 1H, Ar-H), 6.83 (ddd, *J* = 8.5 Hz, 6.9 Hz, 1.2 Hz, 1H, Ar-H), 4.12 (t, *J* = 6.6 Hz, 2H, OCH_2CH_2), 1.89–1.82 (m, 2H, OCH_2CH_2), 1.52–1.44 (m, 2H, CH_2), 1.39–1.31 (m, 4H, CH_2), 0.91 (t, *J* = 7.1 Hz, 3H, CH_3); ^{19}F NMR (470 MHz, $CDCl_3$) δ –145.99 (ddd, *J* = 19.6 Hz, *J* = 7.2, *J* = 1.4 Hz), –159.00 (ddd, *J* = 19.6 Hz, *J* = 6.8, *J* = 2.1 Hz).

2,3-Difluoro-4-n-hexyloxybenzoic acid, **B6F$_{23}$**

Synthesized according to the above procedure described for **B6F$_3$** using 2,3-difluoro-4-*n*-hexyloxybenzaldehyde **(BF$_{23}$)** (1.0 g, 4.1 mmol), $NaOCl_2$ (2.2 g, 24 mmol), resorcinol (0.57 g, 5.1 mmol) and $NaH_2PO_4{\cdot}2H_2O$ (1.5 g, 12.3 mmol); yield 750 mg (2.9 mmol, 71%); Colourless solid; $C_{13}H_{16}F_2O_3$; *M* = 258.26 g/mol; Cr 108 ^oC Iso; ^1H NMR (400 MHz, $CDCl_3$) δ 7.77 (ddd, *J*

= 9.7, 7.7, 2.3 Hz, 1H, Ar-H), 6.79 (ddd, *J* = 8.9, 7.1, 1.7 Hz, 1H, Ar-H), 4.12 (t, *J* = 6.6 Hz, 2H, OC*H*$_2$CH$_2$), 1.93–1.77 (m, 2H, OCH$_2$C*H*$_2$), 1.59–1.27 (m, 6H, CH$_2$), 0.91 (t, *J* = 7.1 Hz, 3H, CH$_3$); ^{13}C NMR (101 MHz, CDCl$_3$) δ 168.2, 153.3, 150.6, 140.2, 127.1, 110.7, 108.3, 69.9, 31.4, 28.8, 25.4, 22.4, 13.9; ^{19}F NMR (378 MHz, CDCl$_3$) δ –132.50 (ddd, *J* = 19.3, 7.6, 1.5 Hz), –158.23 (ddd, *J* = 19.3, 7.0, 2.2 Hz).

1.2.2. Synthesis of **AH** *and* **AF**

The general procedure involved adding a solution of sodium nitrite (2.28 g, 33 mmol, 1.1 eq.) dissolved in 12 ml of water and 25 ml of a 10% potassium hydroxide aqueous solution to the corresponding fluoro-substituted phenol (30 mmol, 1.0 eq.). The solution was cooled to -20 °C using an acetone/dry ice mixture. Subsequently, a cooled solution of 4-aminopyridine (3.30 g, 36 mmol, 1.2 eq.) dissolved in 10 ml of water and 16 ml of concentrated HCl was added dropwise under vigorous stirring over 90 minutes. The reaction temperature was maintained at around -15 °C throughout the process. After the complete addition, the reaction mixture was stirred for an additional 1 hour, followed by the addition of sodium bicarbonate until no effervescence was observed. The resulting solid material was filtered off, washed with distilled water, dried under vacuum, and used without further purification for the next step.

1.2.3. Synthesis of **AH***n and* **AF***n*

Dissolving 2 mmol (1.0 eq.) of the specific 4-hydroxyphenylazopyridine derivatives **AH** or **AF** in 25 ml of DMF, along with the appropriate 1-bromoalkanes (2.4 mmol, 1.2 eq.), K_2CO_3 (6 mmol, 3 eq.), and a catalytic amount of KI, the reaction was agitated for 18 hours at 90°C. After bringing the reaction mixture to room temperature, it was poured into 100 ml of deionized water, resulting in suspension. The suspension was then extracted with ethyl acetate (3 x 50 mL). The mixed organic layers were washed with water and $NaHCO_3$, dried on anhydrous $MgSO_4$, and the solvent was removed under reduced pressure. The desired products were obtained from the crude material using column chromatography with ethyl acetate/*n*-hexane (2:8).

4-(4-Octyloxyphenylazo)pyridine, **AH8**

Orange solid. 80% Yield, m.p. 71 °C. ^{1}H NMR (600 MHz, CDCl$_3$) δ 8.77 (d, *J* = 6.1 Hz, 2H, Ar-H), 7.95 (d, *J* = 9.0 Hz, 2H, Ar-H), 7.67 (d, *J* = 6.1 Hz, 2H, Ar-H), 7.02 (d, *J* = 9.0 Hz, 2H,

Ar-H), 4.06 (t, *J* = 6.6 Hz, 2H, -OC*H*$_2$CH$_2$), 1.86–1.77 (m, 2H, -OCH$_2$C*H*$_2$), 1.56–1.20 (m, 10H, CH$_2$), 0.90 (t, *J* = 7.0 Hz, 3H, CH$_3$). ^{13}C NMR (151 MHz, CDCl$_3$) δ 162.9, 157.5, 151.1, 146.7, 125.6, 116.1, 114.9, 68.5, 31.8, 29.3, 29.2, 29.1, 25.9, 22.6, 14.1.

4-(4-Decyloxyphenylazo)pyridine, **AH10**

Orange solid. 65% Yield, m.p. 66 °C. ^{1}H NMR (600 MHz, CDCl$_3$) δ 8.77 (d, *J* = 6.1 Hz, 2H, Ar-H), 7.95 (d, *J* = 8.9 Hz, 2H, Ar-H), 7.67 (d, *J* = 6.2 Hz, 2H, Ar-H), 7.02 (d, *J* = 8.9 Hz, 2H, Ar-H), 4.06 (t, *J* = 6.6 Hz, 2H, -OC*H*$_2$CH$_2$), 1.87–1.78 (m, 2H, -OCH$_2$C*H*$_2$), 1.52–1.21 (m, 14H, CH$_2$), 0.89 (t, *J* = 7.0 Hz, 3H, CH$_3$). ^{13}C NMR (151 MHz, CDCl$_3$) δ 162.9, 157.5, 151.1, 146.7, 125.6, 116.1, 114.9, 68.5, 31.8, 29.6, 29.5, 29.3, 29.2, 29.1, 25.9, 22.6, 14.1.

4-(4-Dodecyloxyphenylazo)pyridine, **AH12**

Orange solid. 61% Yield, m.p. 73 °C. ^{1}H NMR (600 MHz, CDCl$_3$) δ 8.77 (d, *J* = 6.1 Hz, 2H, Ar-H), 7.95 (d, *J* = 9.0 Hz, 2H, Ar-H), 7.67 (d, *J* = 6.1 Hz, 2H, Ar-H), 7.02 (d, *J* = 9.0 Hz, 2H, Ar-H), 4.06 (t, *J* = 6.6 Hz, 2H, -OC*H*$_2$CH$_2$), 1.87–1.78 (m, 2H, -OCH$_2$C*H*$_2$), 1.53–1.21 (m, 18H, CH$_2$), 0.88 (t, *J* = 7.0 Hz, 3H, CH$_3$).^{13}C NMR (151 MHz, CDCl$_3$) δ 162.9, 157.5, 151.0, 146.7, 125.6, 116.1, 114.9, 68.5, 31.9, 29.6, 29.6, 29.5, 29.5, 29.3, 29.2, 29.1, 25.9, 22.6, 14.1.

4-(4-Tetradeylcoxyphenylazo)pyridine, **AH14**

Orange solid. 65% Yield, m.p. 69 °C. ^{1}H NMR (600 MHz, CDCl$_3$) δ 8.77 (d, *J* = 5.9 Hz, 2H, Ar-H), 7.95 (d, *J* = 9.0 Hz, 2H, Ar-H), 7.67 (d, *J* = 6.0 Hz, 2H, Ar-H), 7.02 (d, *J* = 9.0 Hz, 2H, Ar-H), 4.06 (t, *J* = 6.6 Hz, 2H, -OC*H*$_2$CH$_2$), 1.84–1.80 (m, 2H, -OCH$_2$C*H*$_2$), 1.56–1.12 (m, 22H, CH$_2$), 0.88 (t, *J* = 7.0 Hz, 3H, CH$_3$).^{13}C NMR (151 MHz, CDCl$_3$) δ 162.9, 157.5, 151.0, 146.7, 125.6, 116.1, 114.9, 68.5, 31.9, 29.7, 29.6, 29.6, 29.5, 29.5, 29.3, 29.1, 25.9, 22.6, 14.1.

4-(3-Fluoro-4-octoxyphenylazo)pyridine, **AF8**

Orange crystals. 30% Yield, m.p. 58-59 °C. ^{1}H NMR (500 MHz, CDCl$_3$) δ 8.79 (dd, *J* = 4.5, 1.6 Hz, 2H, Ar-H), 7.82 (ddd, *J* = 8.7, 2.3, 1.3 Hz, 1H, Ar-H), 7.72 (dd, *J* = 11.9, 2.3 Hz, 1H, Ar-H), 7.67 (dd, *J* = 4.5, 1.6 Hz, 2H, Ar-H), 7.09 (t, *J* = 8.6 Hz, 1H, Ar-H), 4.14 (t, *J* = 6.6 Hz, 2H, -OCH$_2$C*H*$_2$), 1.93–1.82 (m, 2H, -OCH$_2$C*H*$_2$), 1.54–1.26 (m, 10H, CH$_2$), 0.89 (t, *J* = 6.9 Hz, 3H, CH$_3$). ^{13}C NMR (126 MHz, CDCl$_3$) δ 157.1, 153.9, 151.9, 151.3, 151.2, 151.1, 146.2, 124.3, 116.1, 113.4, 107.9, 69.6, 31.8, 29.3, 29.2, 29.0, 25.9, 22.6, 14.1. ^{19}F NMR (470 MHz, CDCl$_3$) δ - 132.39 (dd, *J* = 11.6, 8.7 Hz).

4-(3-Fluoro-4-decoxyphenylazo)pyridine, **AF10**

Orange crystals. 35% Yield, m.p. 57-58 °C. ^{1}H NMR (500 MHz, $CDCl_3$) δ 8.79 (dd, *J* = 4.5, 1.6 Hz, 2H, Ar-H), 7.82 (ddd, *J* = 8.7, 2.4, 1.2 Hz, 1H, Ar-H), 7.72 (dd, *J* = 11.9, 2.3 Hz, 1H, Ar-H), 7.67 (dd, *J* = 4.5, 1.6 Hz, 2H, Ar-H), 7.09 (t, *J* = 8.6 Hz, 1H, Ar-H), 4.14 (t, *J* = 6.6 Hz, 2H, -OC*H*$_2$CH$_2$), 2.01–1.76 (m, 2H, -OCH$_2$C*H*$_2$), 1.60–1.18 (m, 14H, CH_2), 0.90–0.87 (m, 3H, CH_3). ^{13}C NMR (126 MHz, $CDCl_3$) δ 157.1, 153.8, 151.9, 151.3, 151.2, 151.1, 146.2, 124.3, 116.1, 113.4, 107.9, 69.6, 31.8-22.6 (m, 8C), 14.1. ^{19}F NMR (470 MHz, $CDCl_3$) δ - 132.40 (dd, *J* = 11.6, 8.6 Hz).

4-(3-Fluoro-4-dodecoxyphenylazo)pyridine, **AF12**

Orange crystals. 29% Yield, m.p. 66-67 °C. ^{1}H NMR (500 MHz, $CDCl_3$) δ 8.79 (dd, *J* = 4.5, 1.6 Hz, 2H, Ar-H), 7.82 (ddd, *J* = 8.7, 2.2, 1.2 Hz, 1H, Ar-H), 7.72 (dd, *J* = 11.9, 2.3 Hz, 1H, Ar-H), 7.67 (dd, *J* = 4.5, 1.6 Hz, 2H, Ar-H), 7.09 (t, *J* = 8.6 Hz, 1H, Ar-H), 4.14 (t, *J* = 6.6 Hz, 2H, -OC*H*$_2$CH$_2$), 1.94–1.79 (m, 2H, -OCH$_2$C*H*$_2$), 1.55–1.20 (m, 18H, CH_2), 0.88 (t, *J* = 6.9 Hz, 3H, CH_3). ^{13}C NMR (126 MHz, $CDCl_3$) δ 157.1, 153.9, 151.9, 151.3, 151.2, 151.1, 146.2, 124.2, 116.1, 113.3, 107.9, 69.5, 31.9, 29.7, 29.6, 29.5, 29.4, 29.3, 29.3, 29.0, 25.8, 22.6, 14.1. ^{19}F NMR (470 MHz, $CDCl_3$) δ - 132.38 (dd, *J* = 11.6, 8.7 Hz).

4-(3-Fluoro-4-tetradecoxyphenylazo)pyridine, **AF14**

Orange crystals. 25% Yield, m.p. 68-69 °C. ^{1}H NMR (500 MHz, $CDCl_3$) δ 8.79 (dd, *J* = 4.5, 1.6 Hz, 2H, Ar-H), 7.82 (ddd, *J* = 8.7, 2.3, 1.3 Hz, 1H, Ar-H), 7.72 (dd, *J* = 11.9, 2.3 Hz, 1H, Ar-H), 7.67 (dd, *J* = 4.5, 1.6 Hz, 2H, Ar-H), 7.09 (t, *J* = 8.6 Hz, 1H, Ar-H), 4.14 (t, *J* = 6.6 Hz, 2H, -OC*H*$_2$CH$_2$), 1.95– 1.79 (m, 2H, -OCH$_2$C*H*$_2$), 1.56–1.15 (m, 22H, CH_2), 0.88 (t, *J* = 7.0 Hz, 3H, CH_3). ^{13}C NMR (126 MHz, $CDCl_3$) δ 157.1, 153.8, 151.9, 151.3, 151.2, 151.1, 146.2, 124.3, 116.1, 113.4, 107.9, 69.6, 31.9, 29.7-29.3 (m, 8C), 29.0, 25.9, 22.7, 14.1. ^{19}F NMR (470 MHz, $CDCl_3$) δ - 132.38 (dd, *J* = 11.7, 8.6 Hz).

*1.2.4. Preparation of final HBCLs supramolecules (***HHH*n* - FFF*n*)**

The target HBLCs (**HHH*n* - FFF*n***) were formed by melting the acid (**B23H6**, **B2F6**, **B3F6** or **B23F6**) and each azopyridine derivatives (**AH*n*** or **AF*n***) in equimolar ratios (1:1) together for few seconds with stirring, resulting in the formation of a homogeneous mixture. The resulting mixture was then allowed to cool to ambient temperature, yielding an orange solid substance. The formed solid was melted once again to ensure the complexation. All complexes exhibited

homogeneous melting and reproducible phase transition temperatures during DSC investigations, indicating the formation of stable hydrogen-bonded supramolecules (see **Figure 2** as examples for DSC traces).

2. NMR Charts

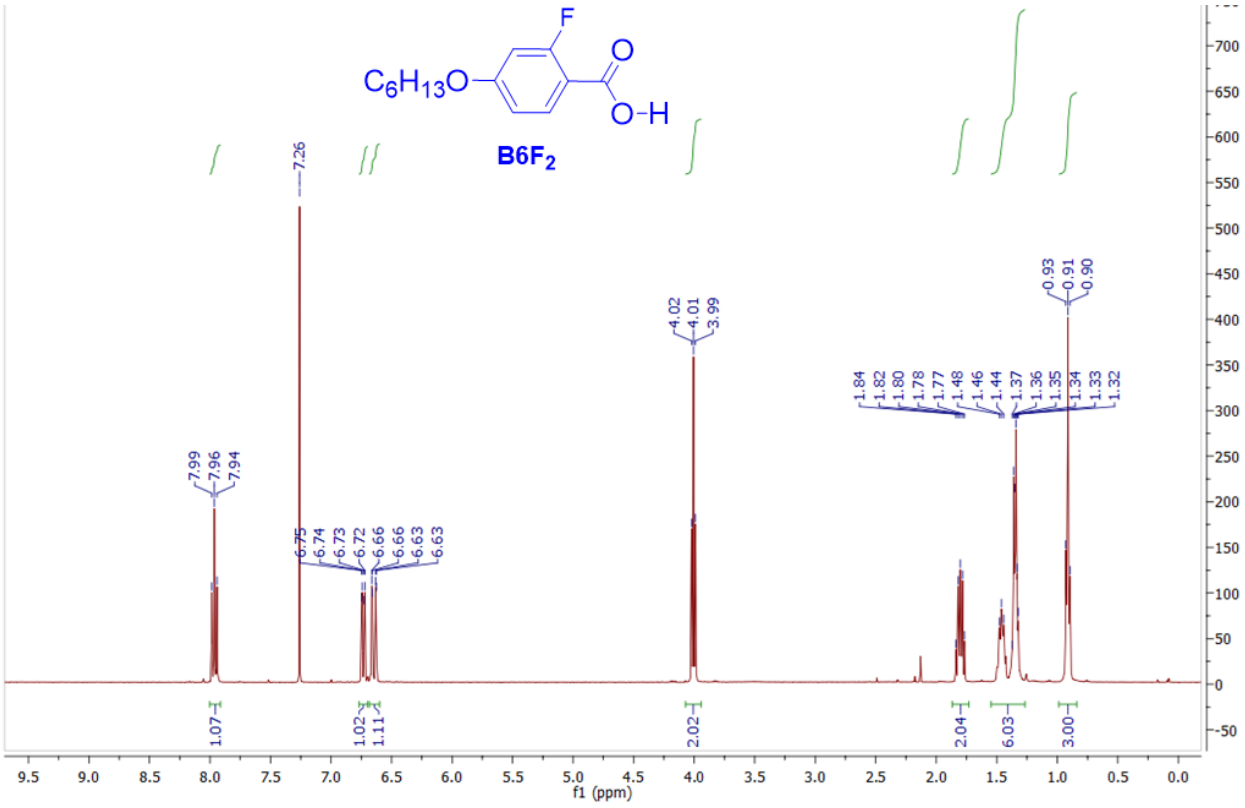

Figure S1a. ^{1}H NMR of compound **B6F$_2$**.

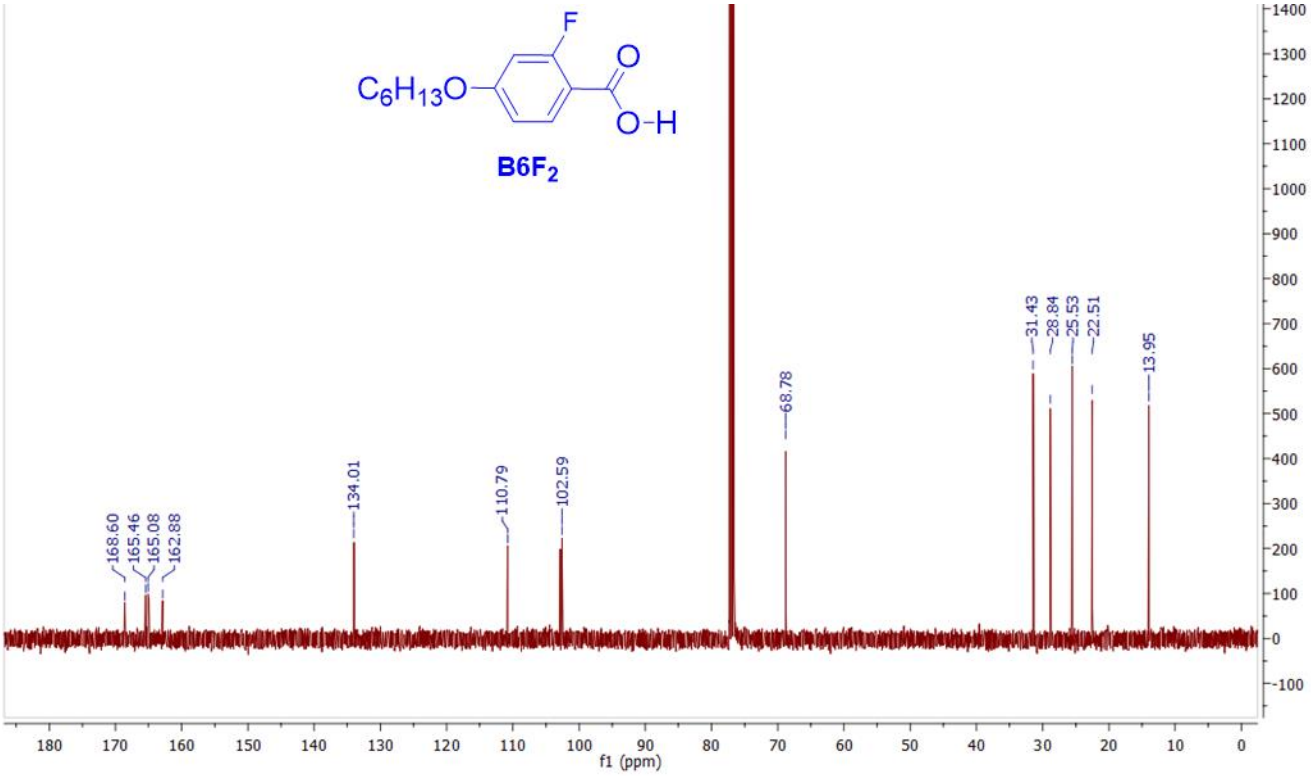

Figure S1b. ^{13}C NMR of compound **B6F$_2$**.

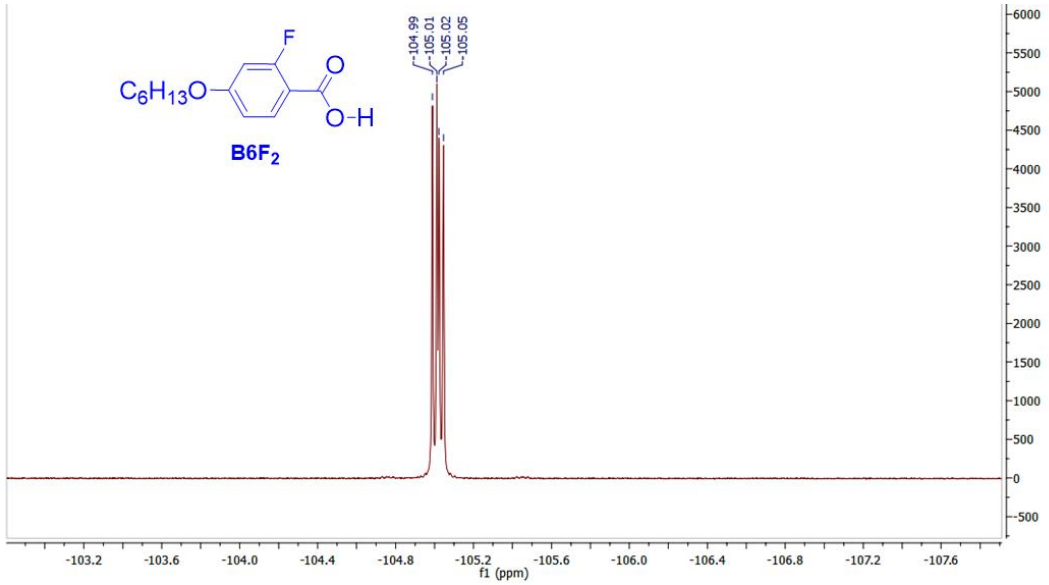

Figure S1c. ^{19}F NMR of compound **B6F$_2$**.

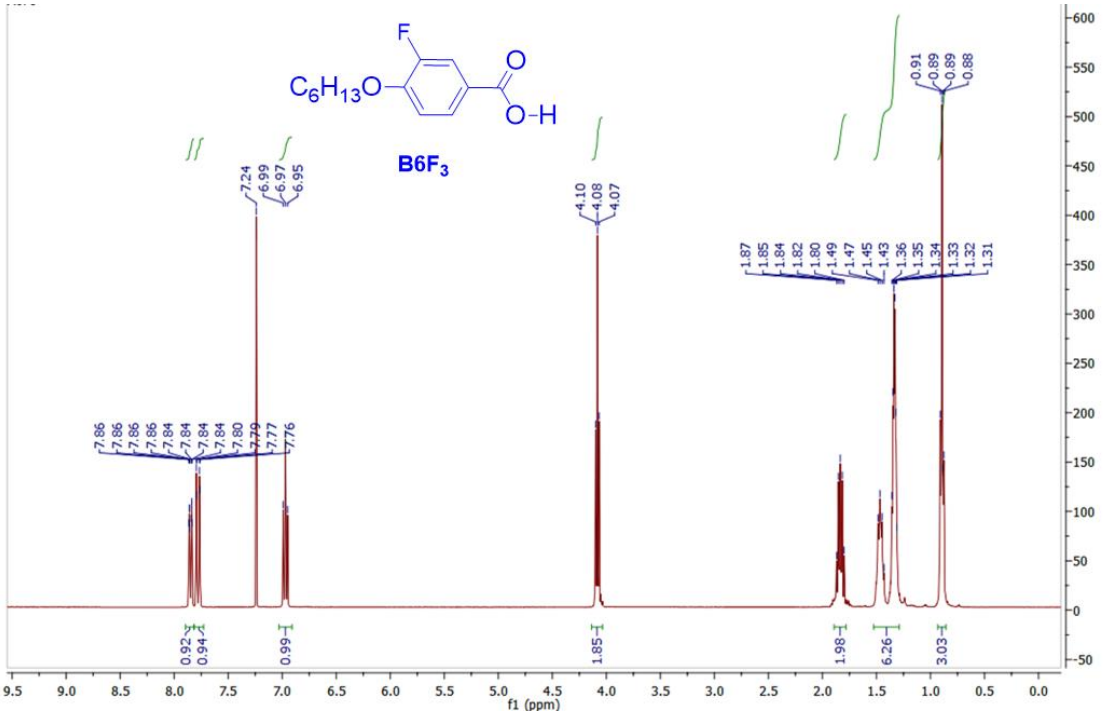

Figure S2a. ^{1}H NMR of compound **B6F$_3$**.

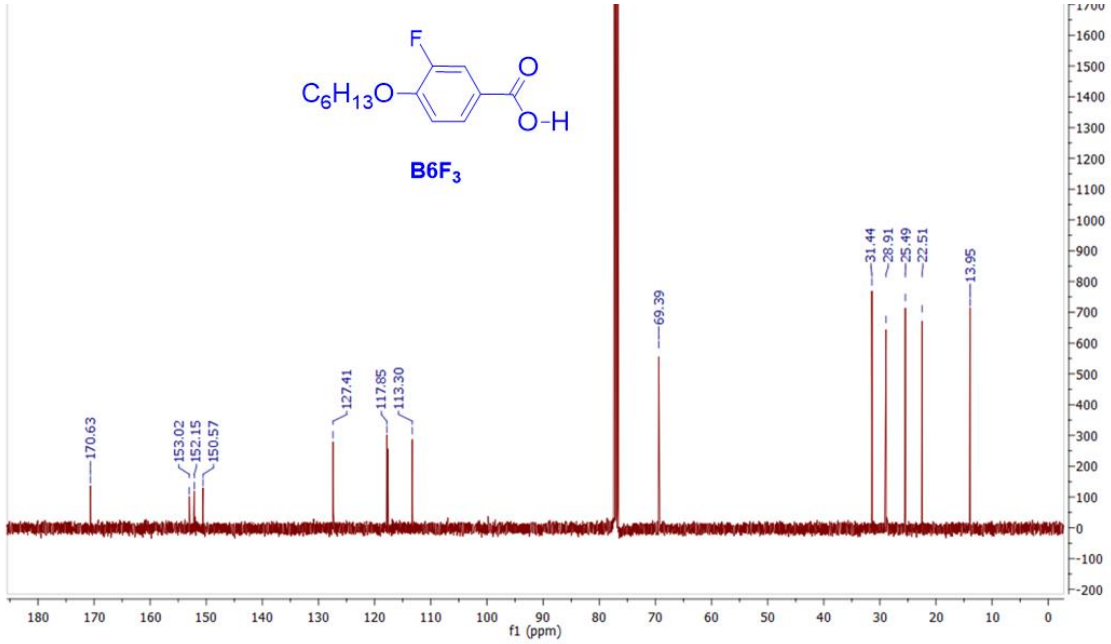

Figure S2b. ^{13}C NMR of compound **B6F$_3$**.

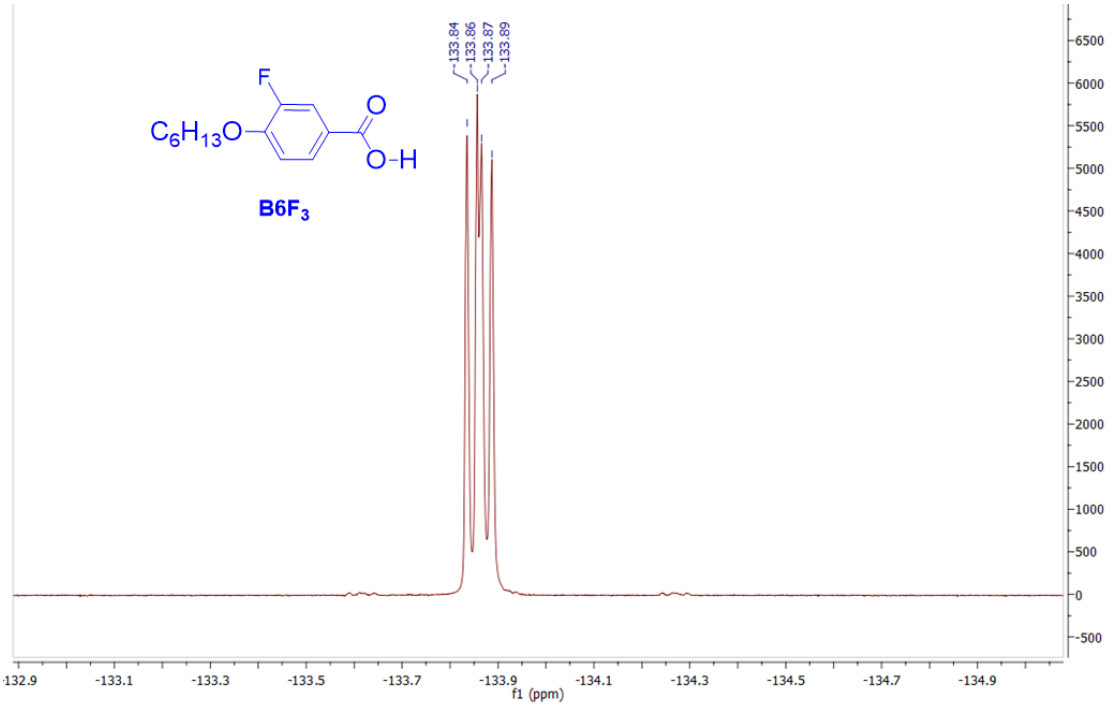

Figure S2c. ^{19}F NMR of compound **B6F$_3$**.

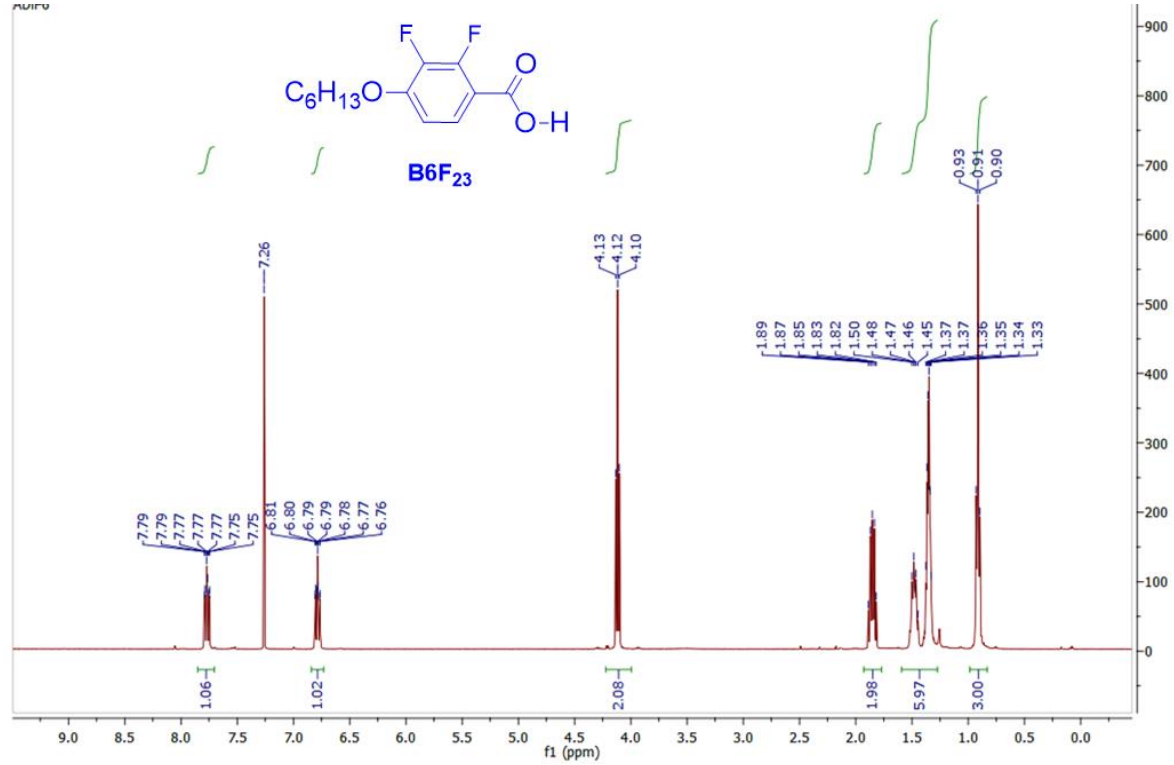

Figure S3a. ^{1}H NMR of compound **B6F$_{23}$**.

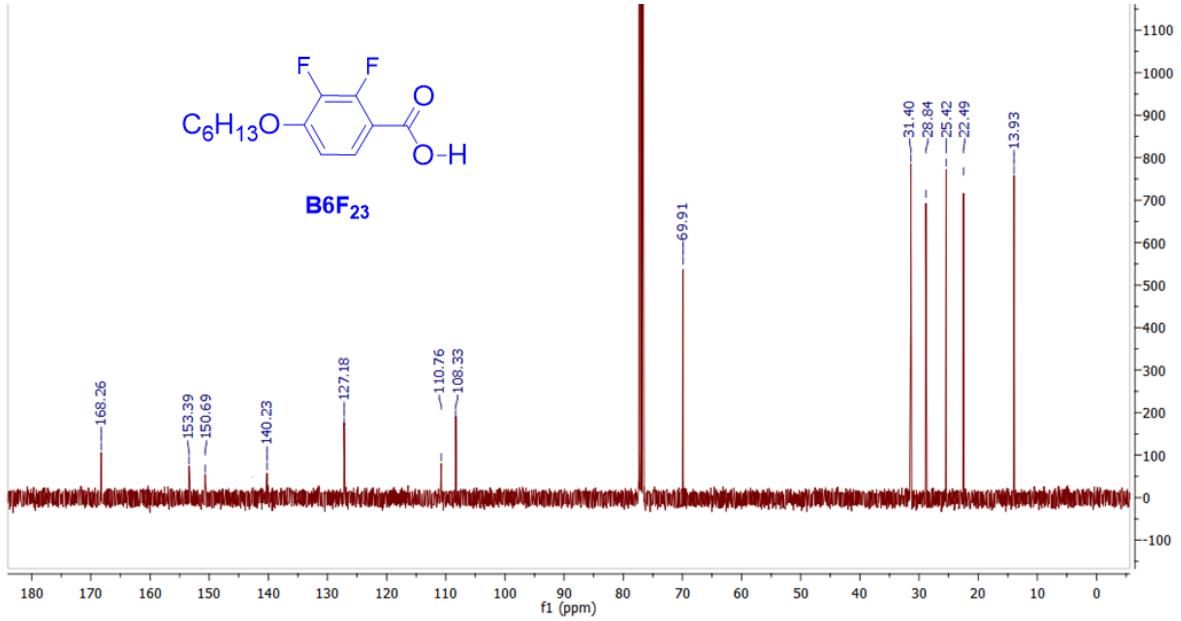

Figure S3b. ^{13}C NMR of compound **B6F$_{23}$**.

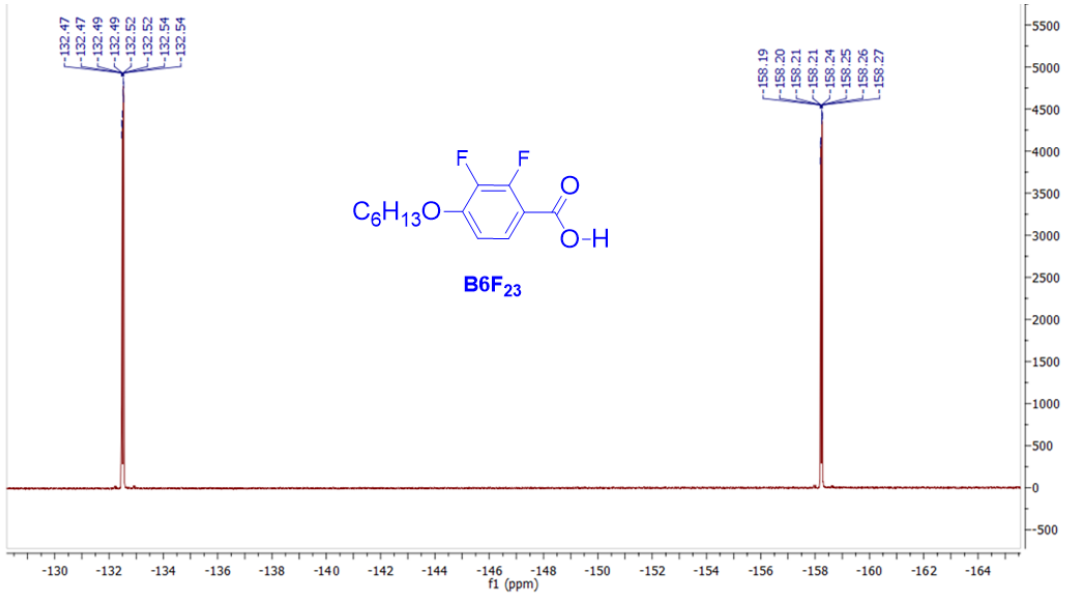

Figure S3c. ^{19}F NMR of compound **B6F$_{23}$**.

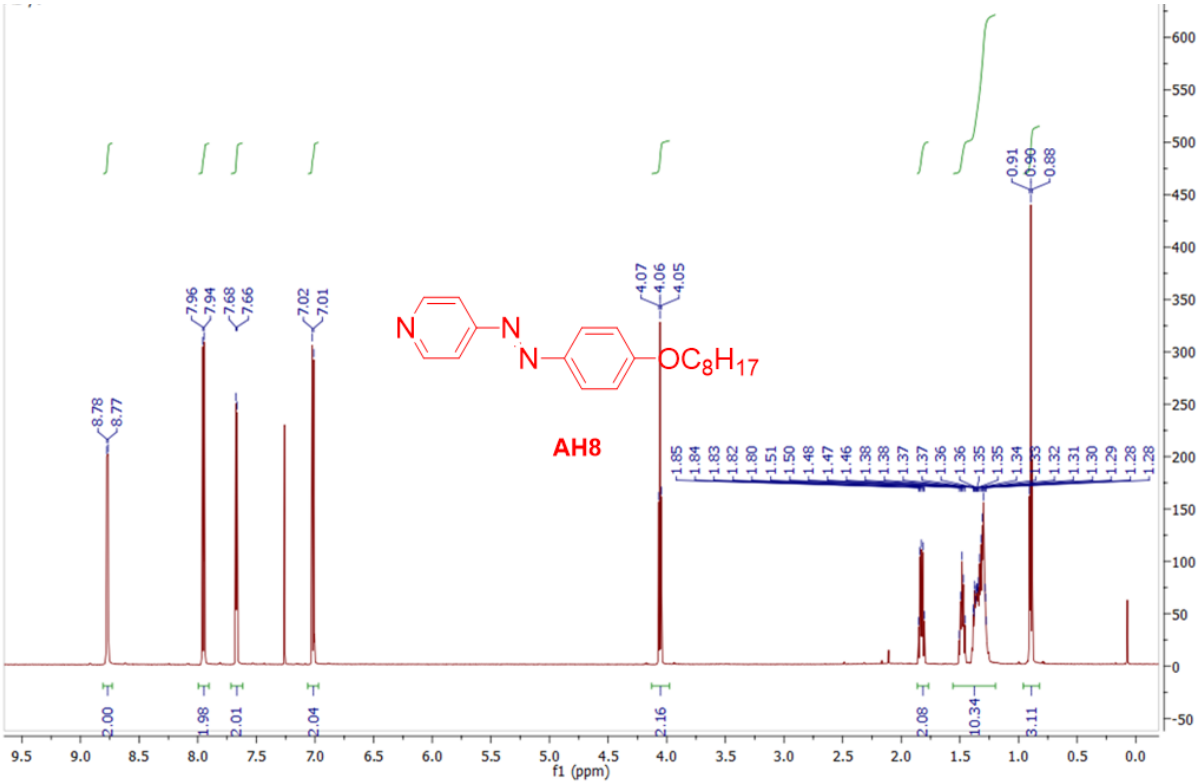

Figure S4a. ^{1}H NMR of compound **AH8**.

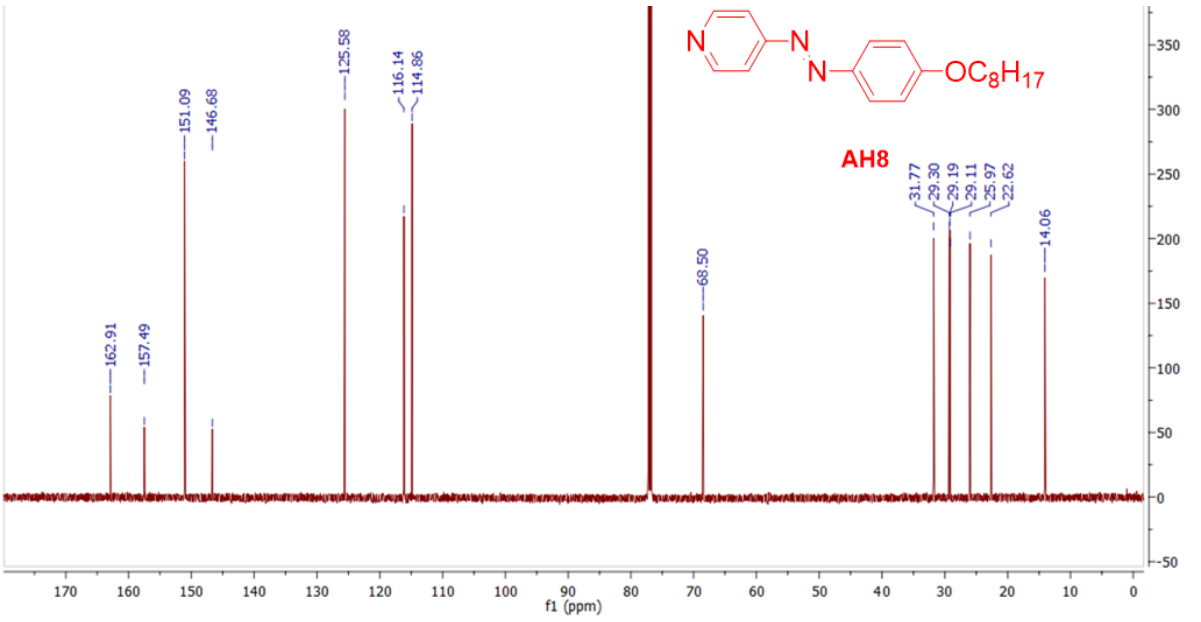

Figure S4b. ^{13}C NMR of compound **AH8**.

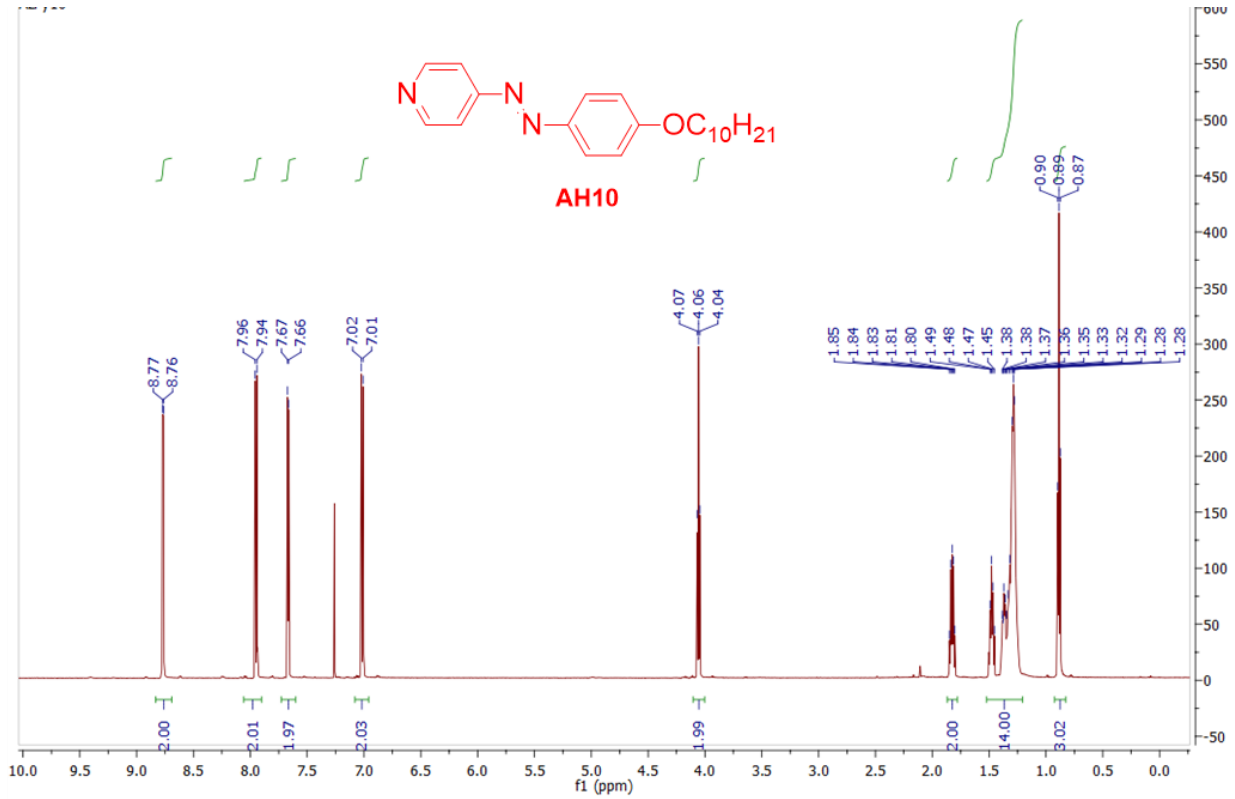

Figure S5a. ^{1}H NMR of compound **AH10**.

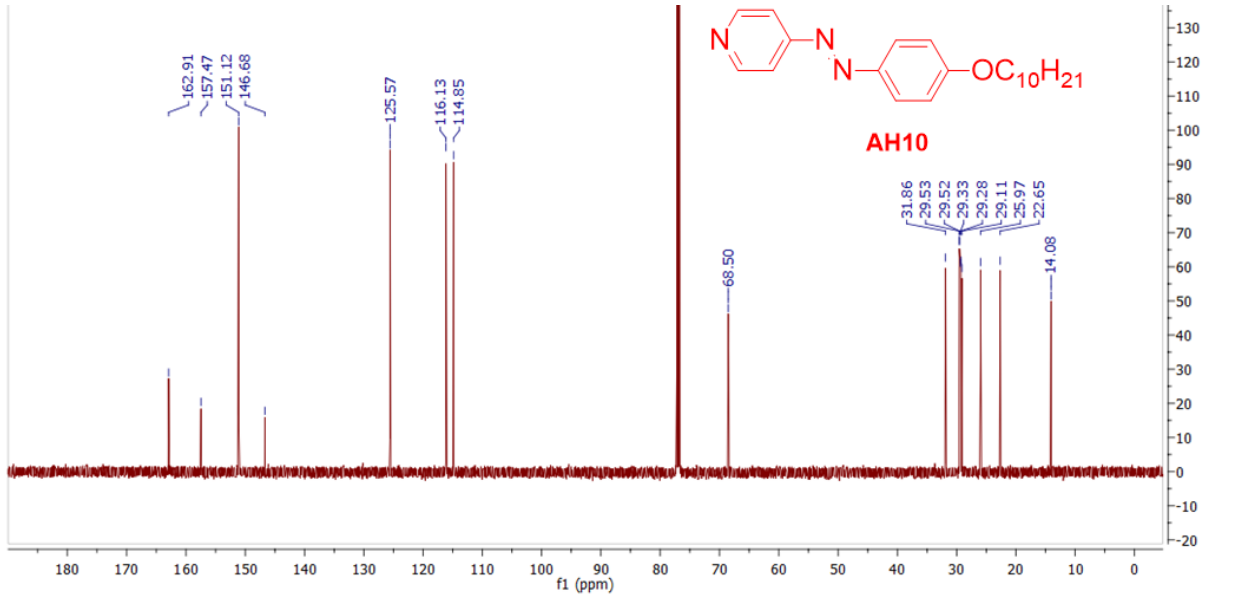

Figure S5b. ^{13}C NMR of compound **AH10**.

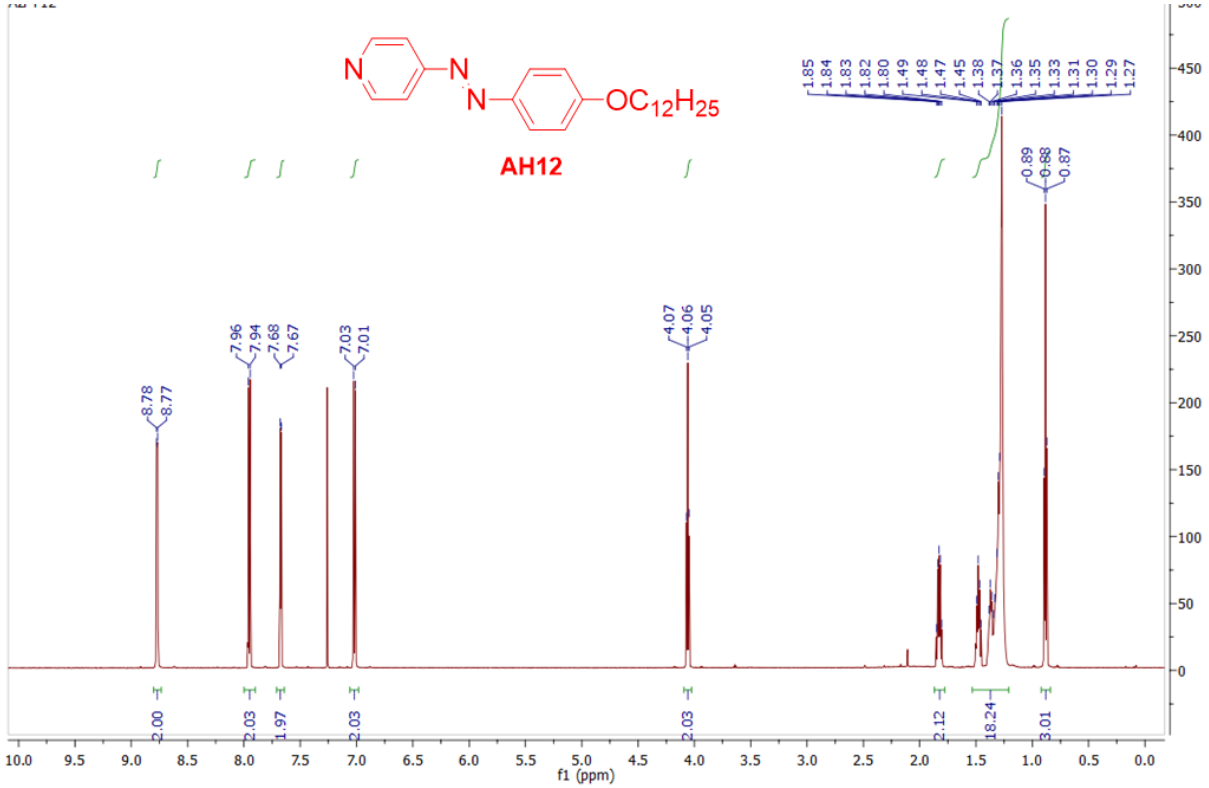

Figure S6a. ^{1}H NMR of compound **AH12**.

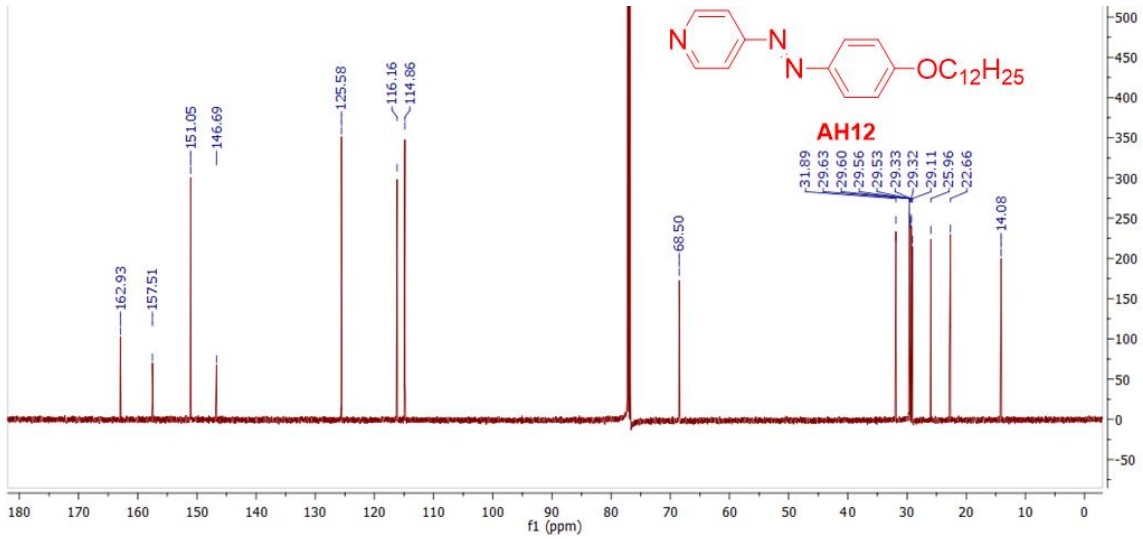

Figure S6b. ^{13}C NMR of compound **AH12**.

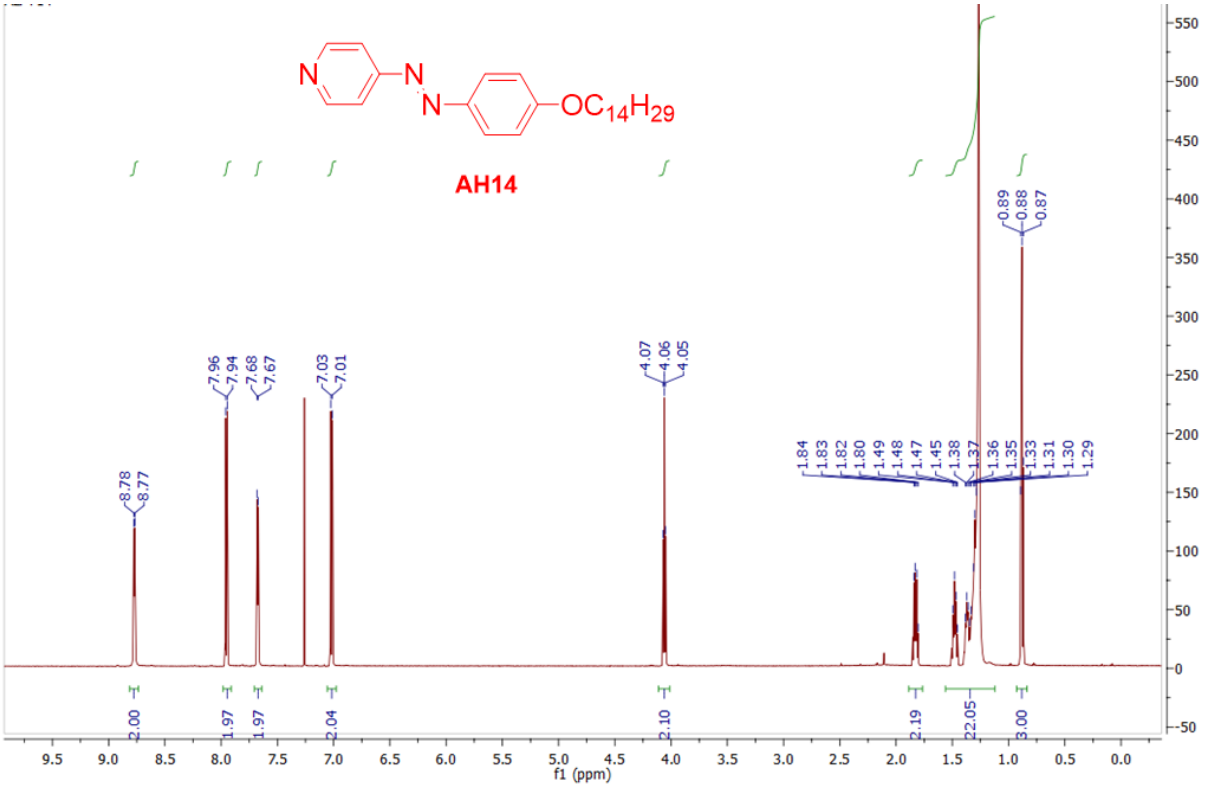

Figure S7a. ^{1}H NMR of compound **AH14**.

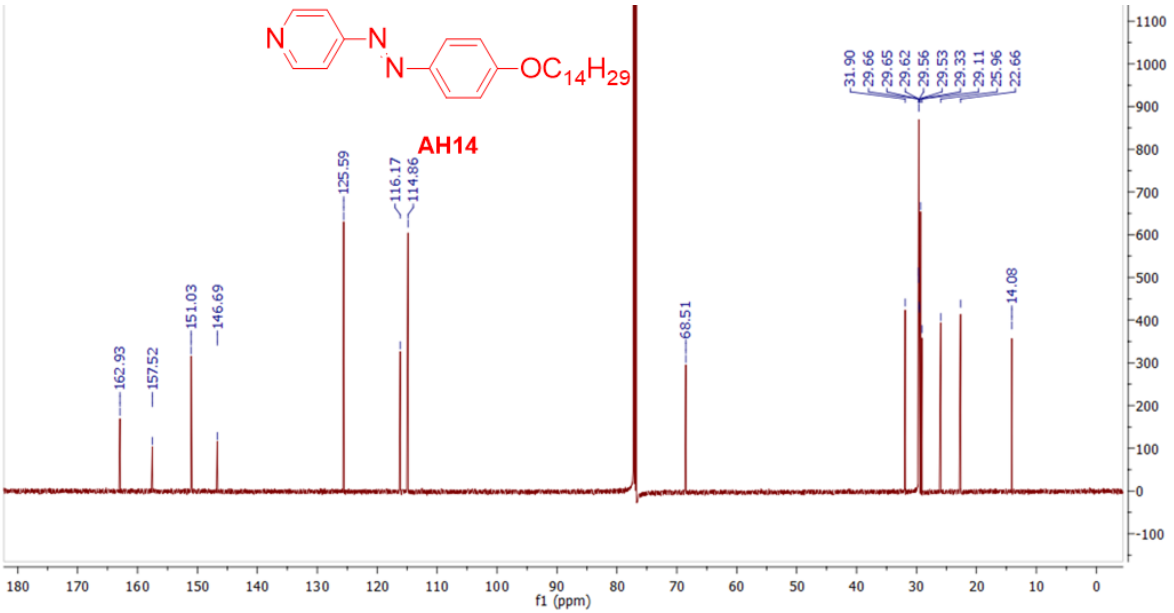

Figure S7b. ^{13}C NMR of compound **AH14**.

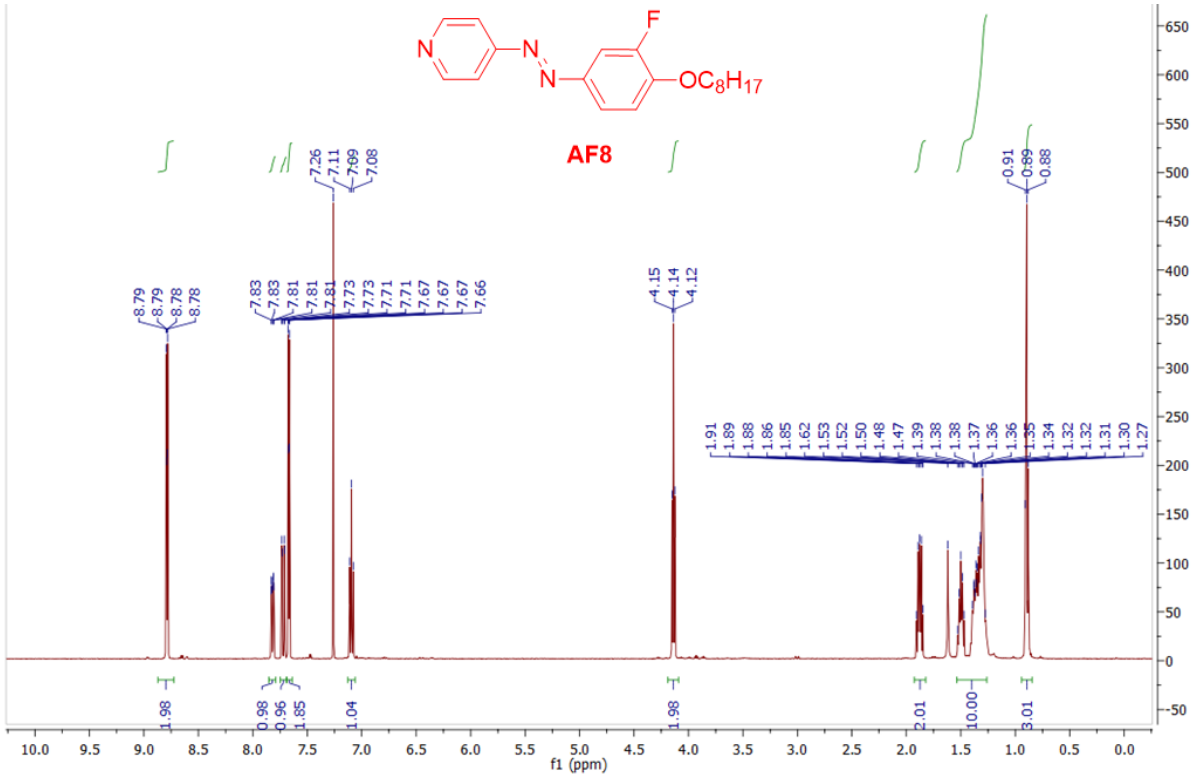

Figure S8a. ^{1}H NMR of compound **AF8**.

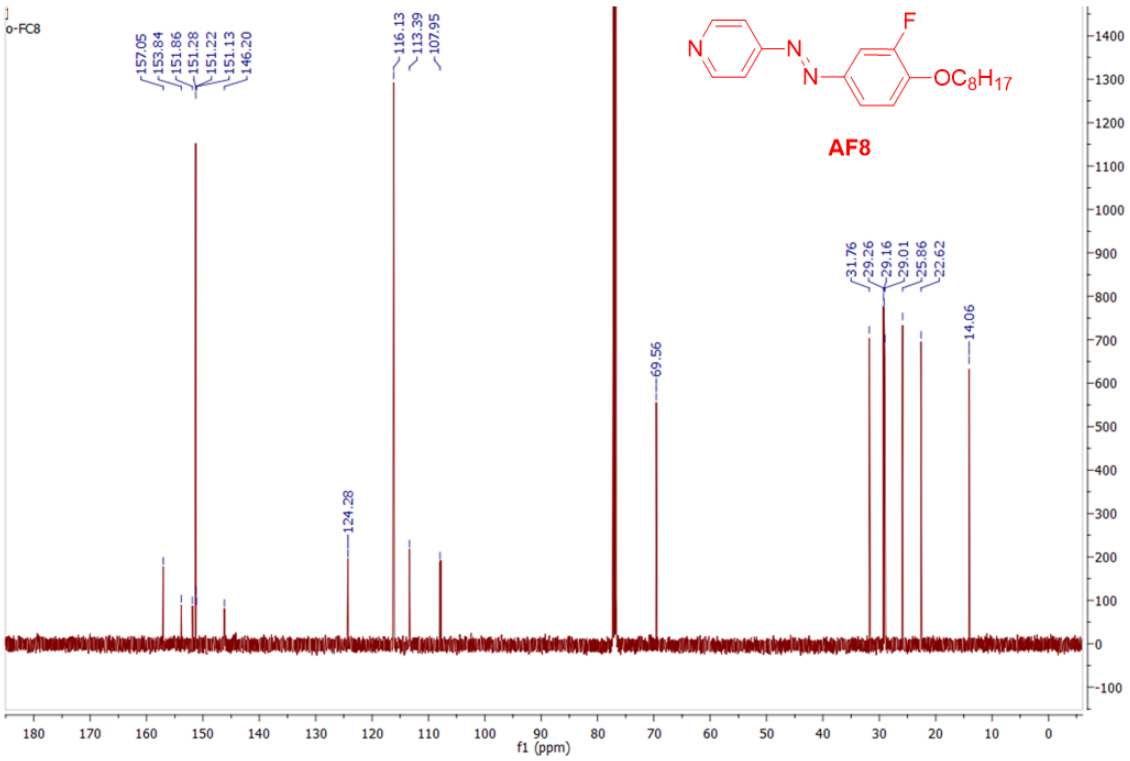

Figure S8b. ^{13}C NMR of compound **AF8**.

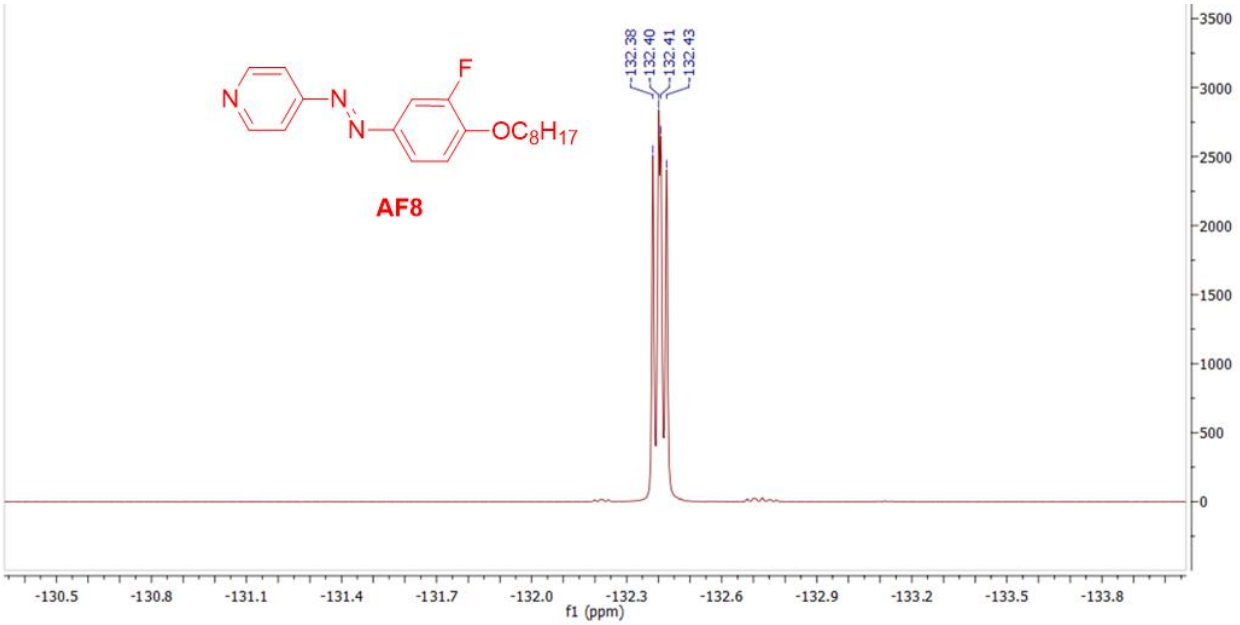

Figure S8c. ^{19}F NMR of compound **AF8**.

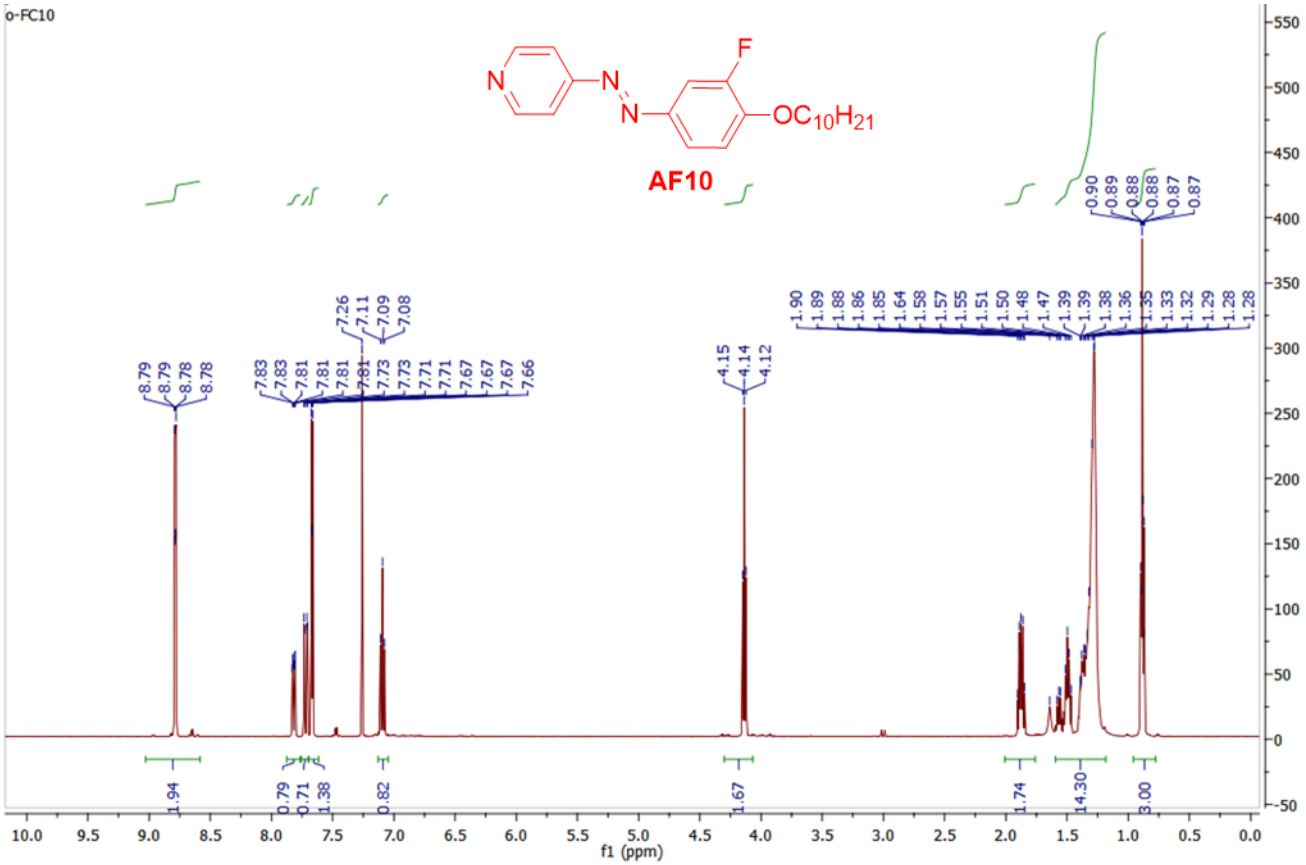

Figure S9a. ^{1}H NMR of compound **AF10**.

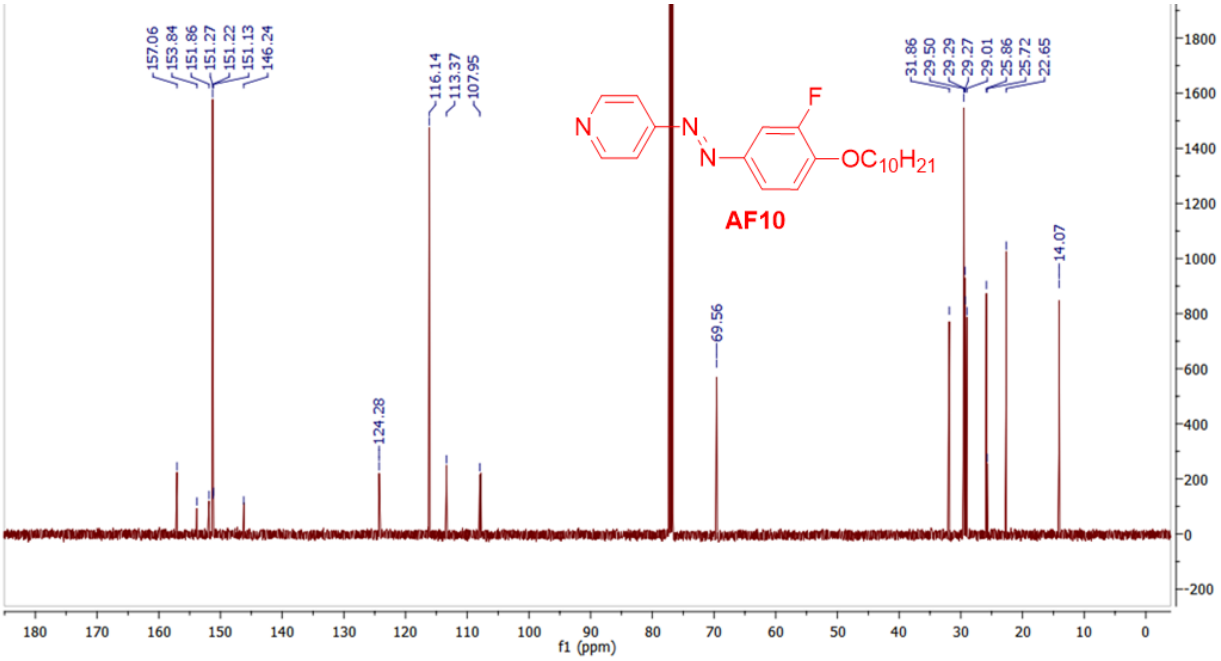

Figure S9b. ^{13}C NMR of compound **AF10**.

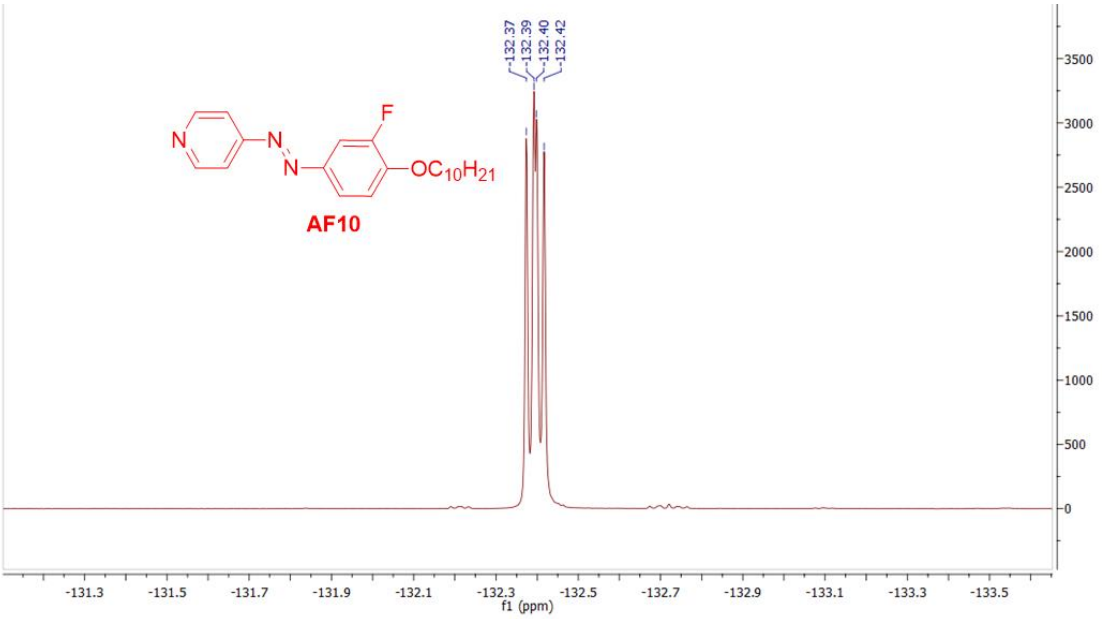

Figure S9c. ^{19}F NMR of compound **AF10**.

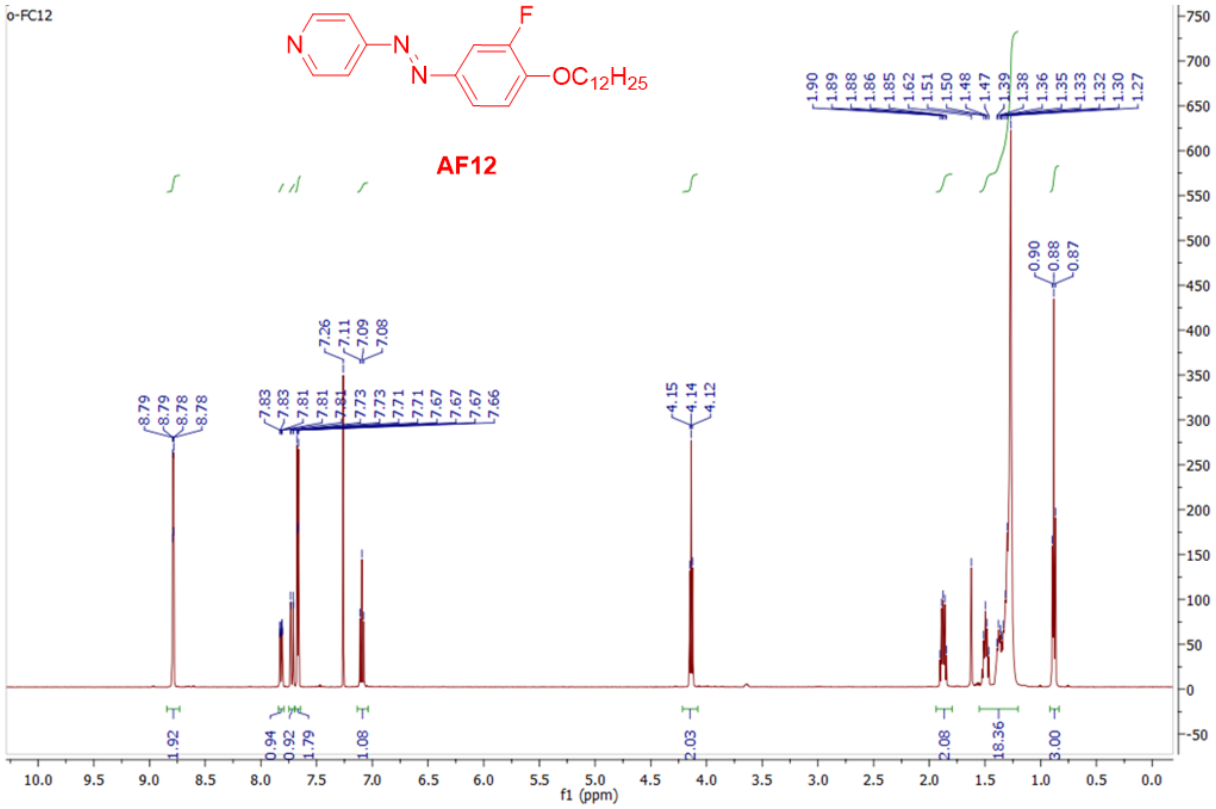

Figure S10a. [1]H NMR of compound **AF12**.

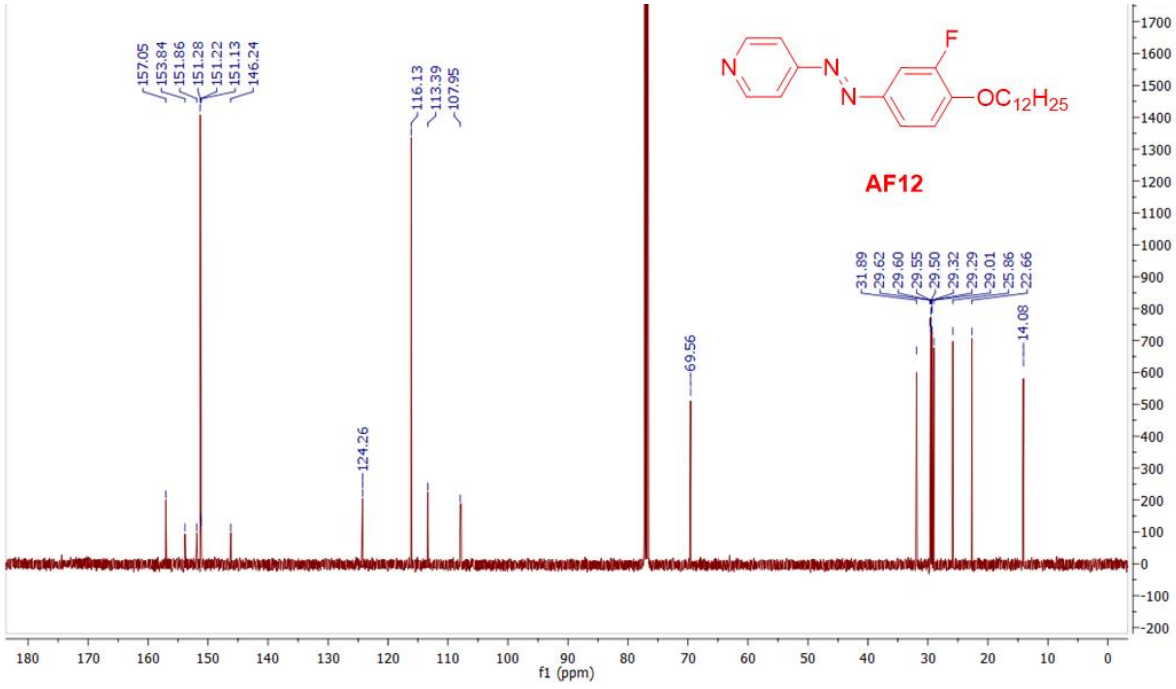

Figure S10b. [13]C NMR of compound **AF12**.

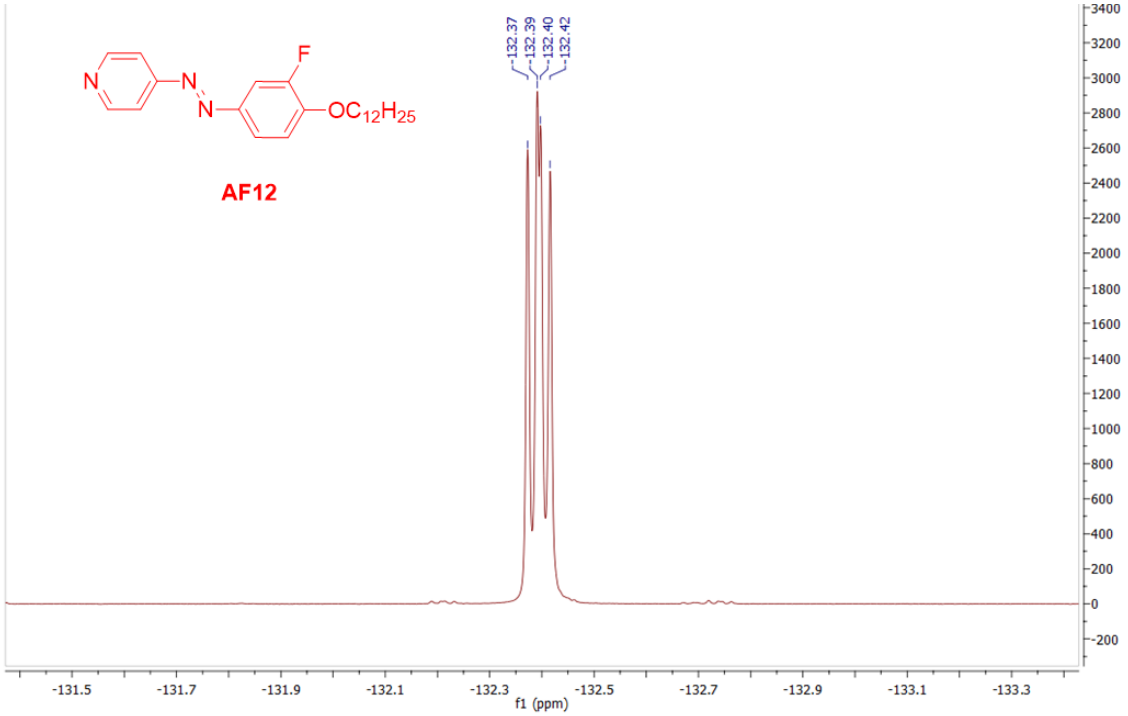

Figure S10c. ^{19}F NMR of compound **AF12**.

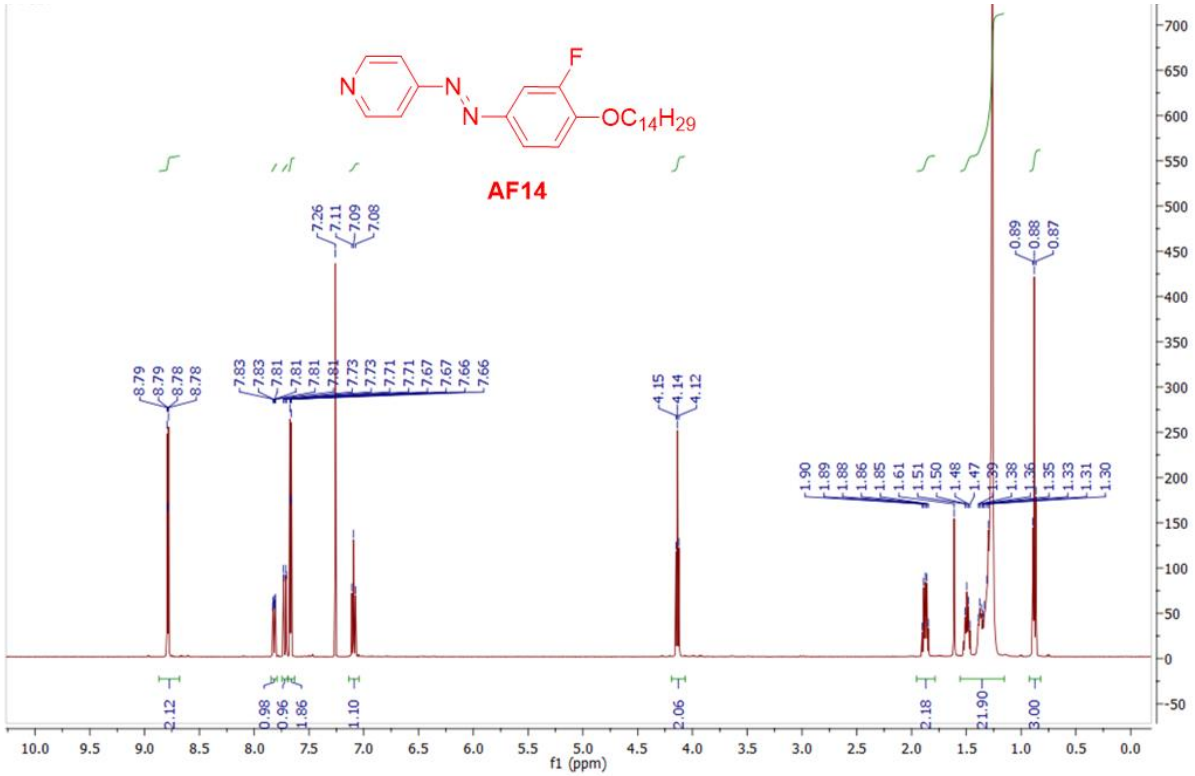

Figure S11a. ^{1}H NMR of compound **AF14**.

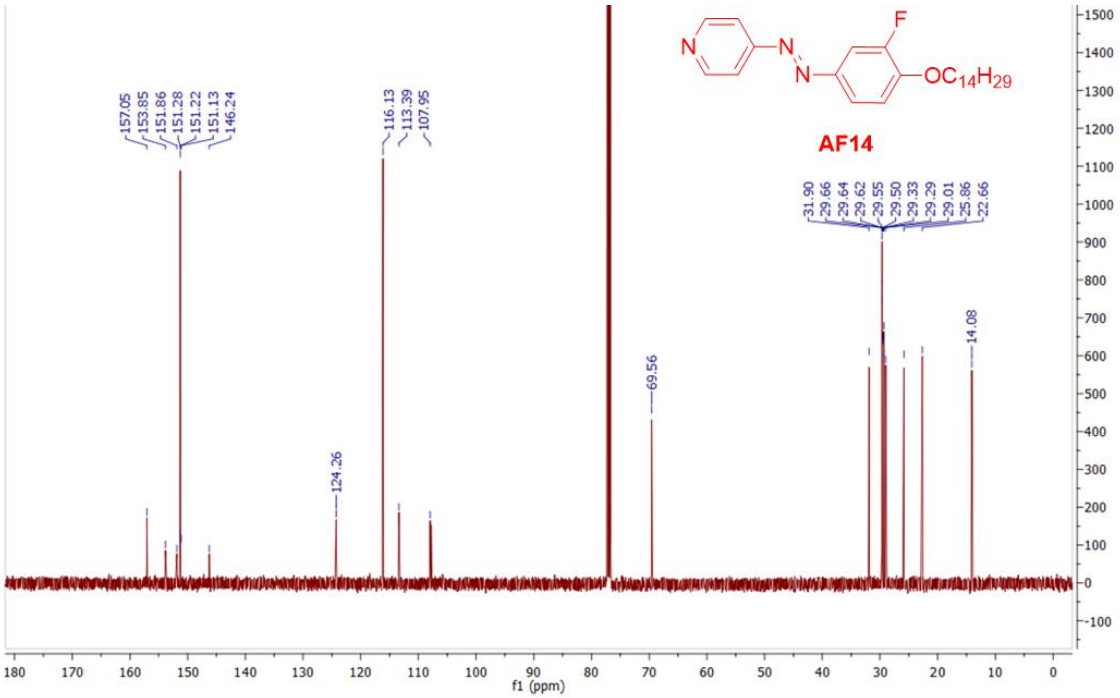

Figure S11b. ^{13}C NMR of compound **AF14**.

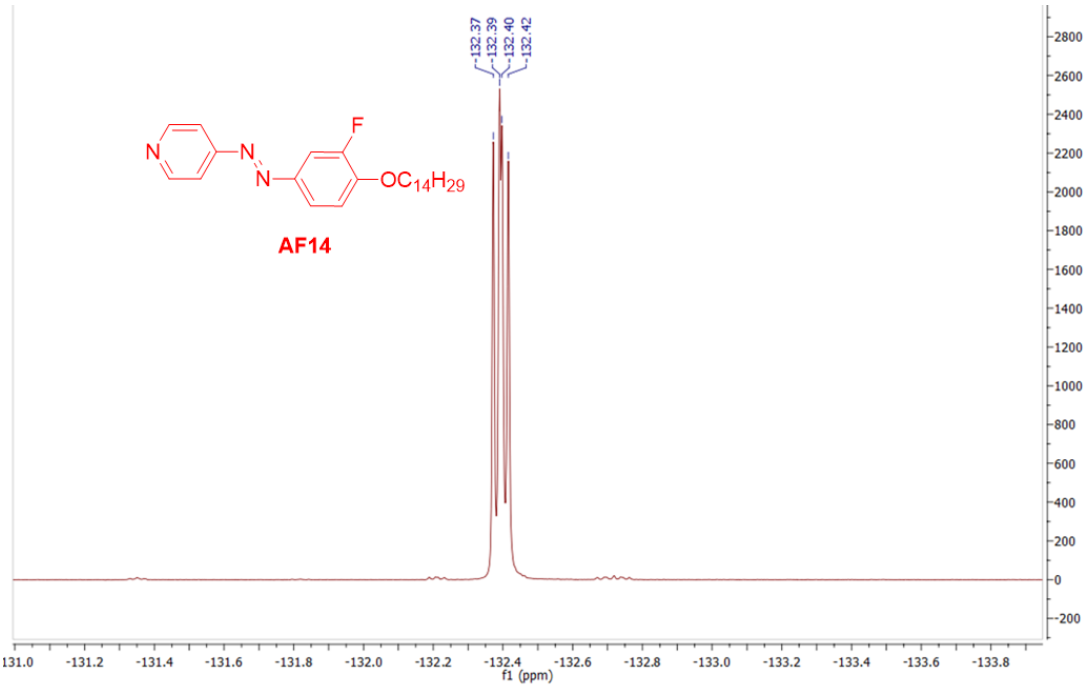

Figure S11c. ^{19}F NMR of compound **AF14**.

3. IR Charts of hydrogen-bonded supramolecules

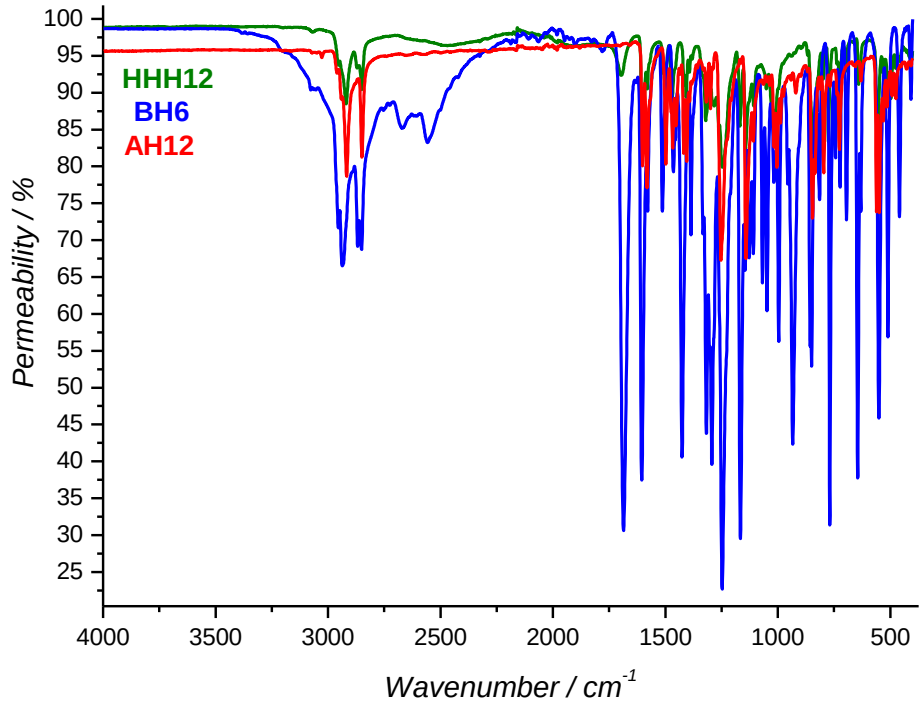

Figure S12a. FTIR spectra of the supramolecule **HHH12** (green) and its complementary components **B6H** (blue), **AH12** (red) in the crystalline state (KBr) at room temperature.

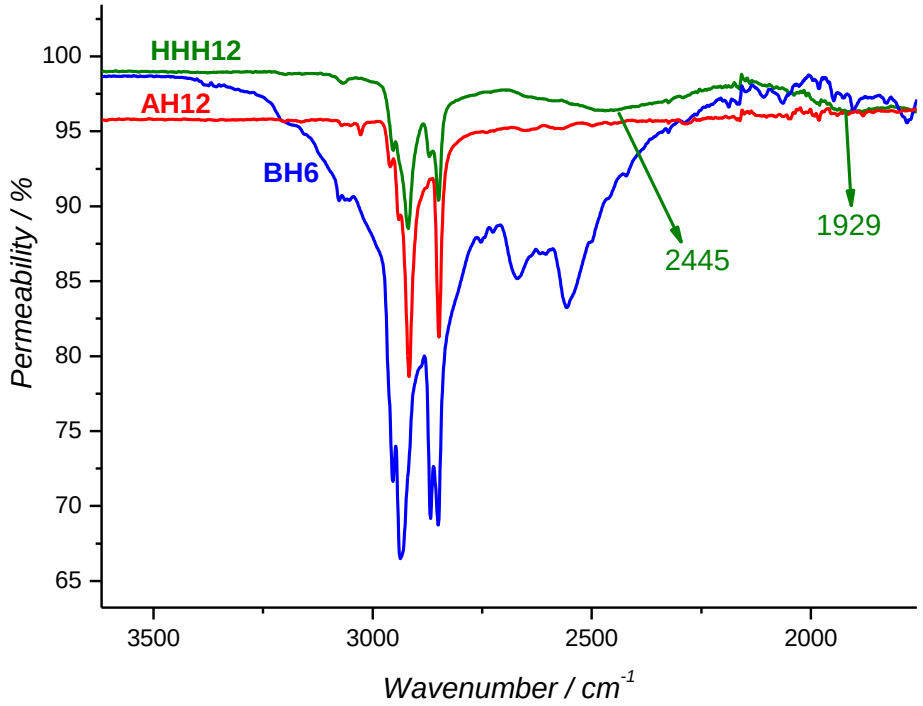

Figure S12b. FTIR spectra of the supramolecule **HHH12** (green) and its complementary components **B6H** (blue), **AH12** (red) in the crystalline state at room temperature enlarged area between 1750 $cm^{-1}$and 3500 cm^{-1}

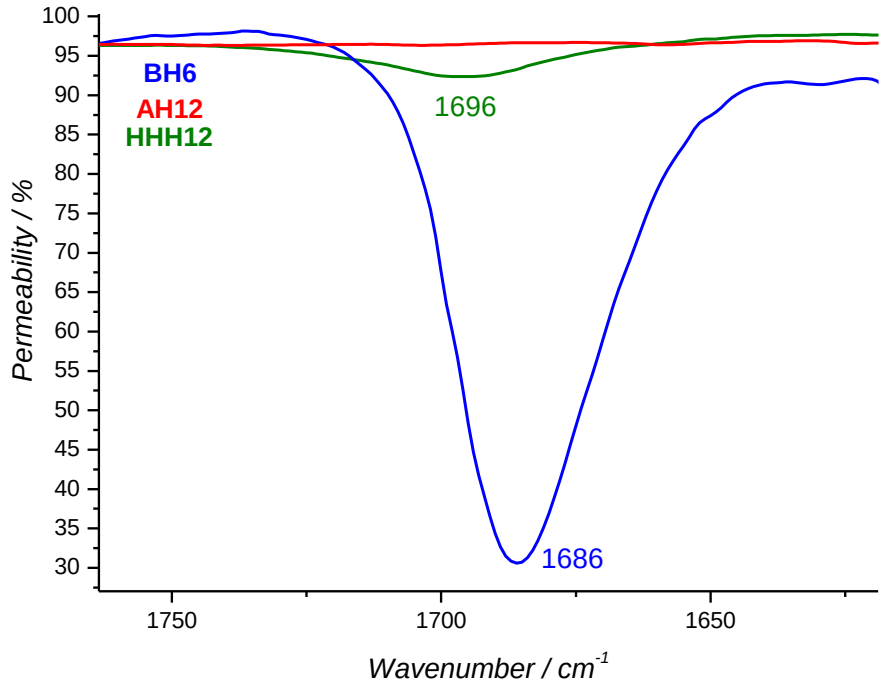

Figure S12c. FTIR spectra of the supramolecule **HHH12** (green) and its complementary components **B6H** (blue), **AH12** (red) in the crystalline state at room temperature enlarged area between 1620 $cm^{-1}$and 1750 cm^{-1}

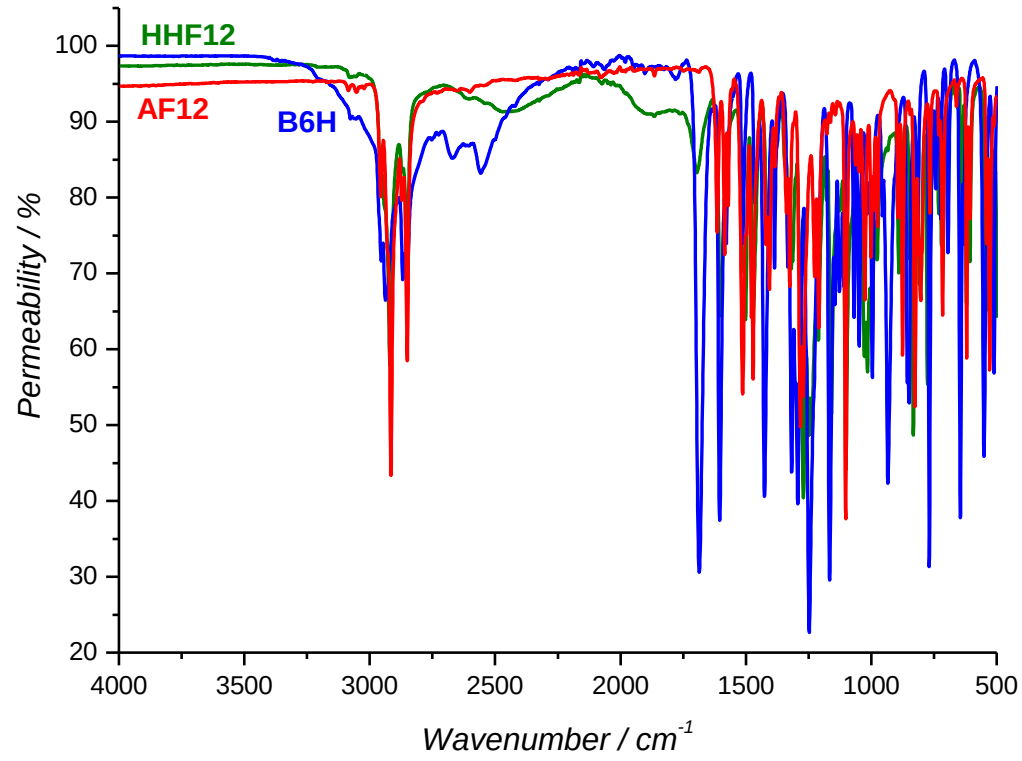

Figure S13a. FTIR spectra of the supramolecule **HHF12** (green) and its complementary components **B6H** (blue), **AF12** (red) in the crystalline state (KBr) at room temperature.

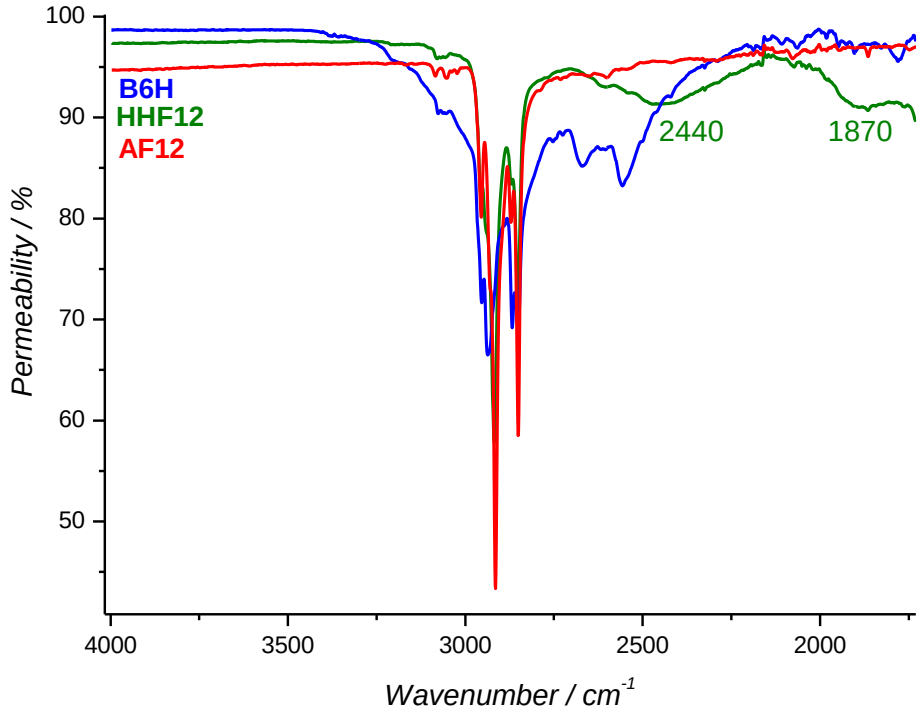

Figure S13b. FTIR spectra of the supramolecule **HHF12** (green) and its complementary components **B6H** (blue), **AF12** (red) in the crystalline state at room temperature enlarged area between 1750 $cm^{-1}$and 4000 cm^{-1}

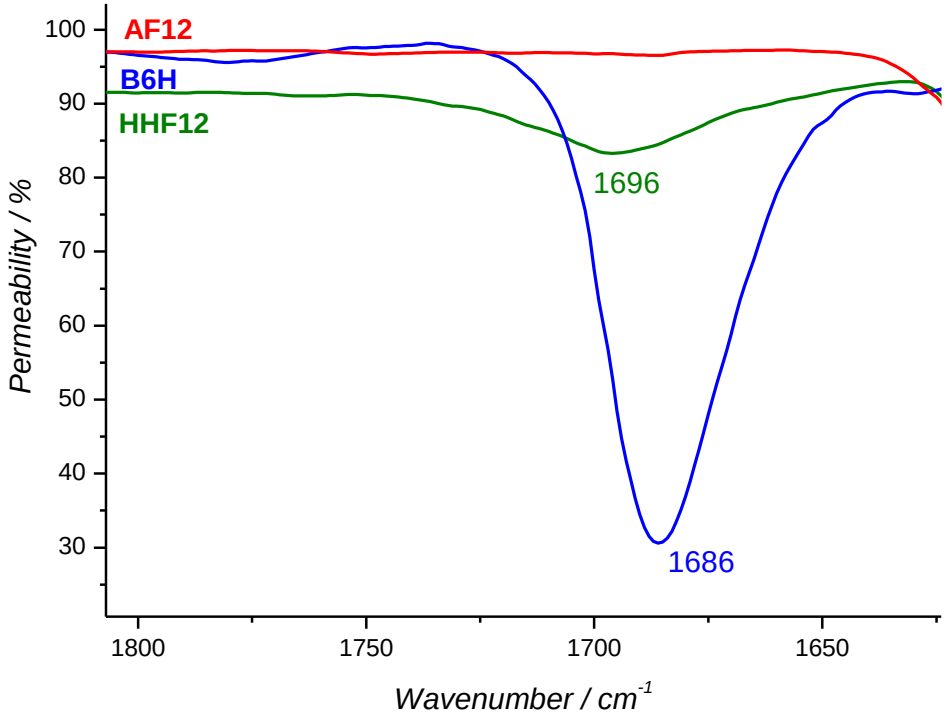

Figure S13c. FTIR spectra of the supramolecule **HHF12** (green) and its complementary components **B6H** (blue), **AF12** (red) in the crystalline state at room temperature enlarged area between 1600 $cm^{-1}$and 1800 cm^{-1}

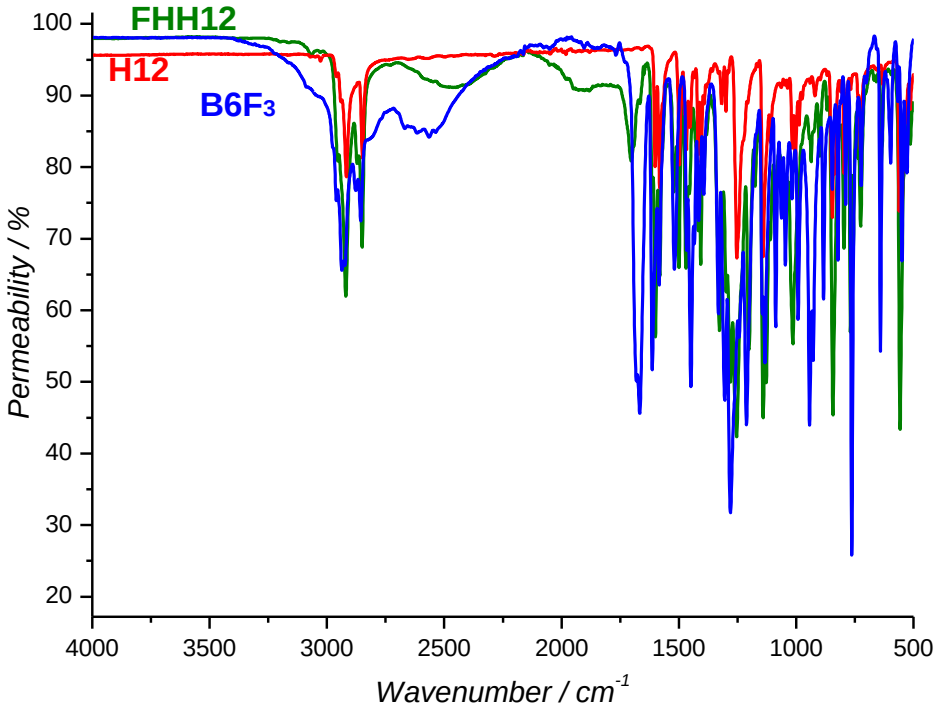

Figure S14a. FTIR spectra of the supramolecule **FHH12** (green) and its complementary components **B6F3** (blue), **AH12** (red) in the crystalline state (KBr) at room temperature.

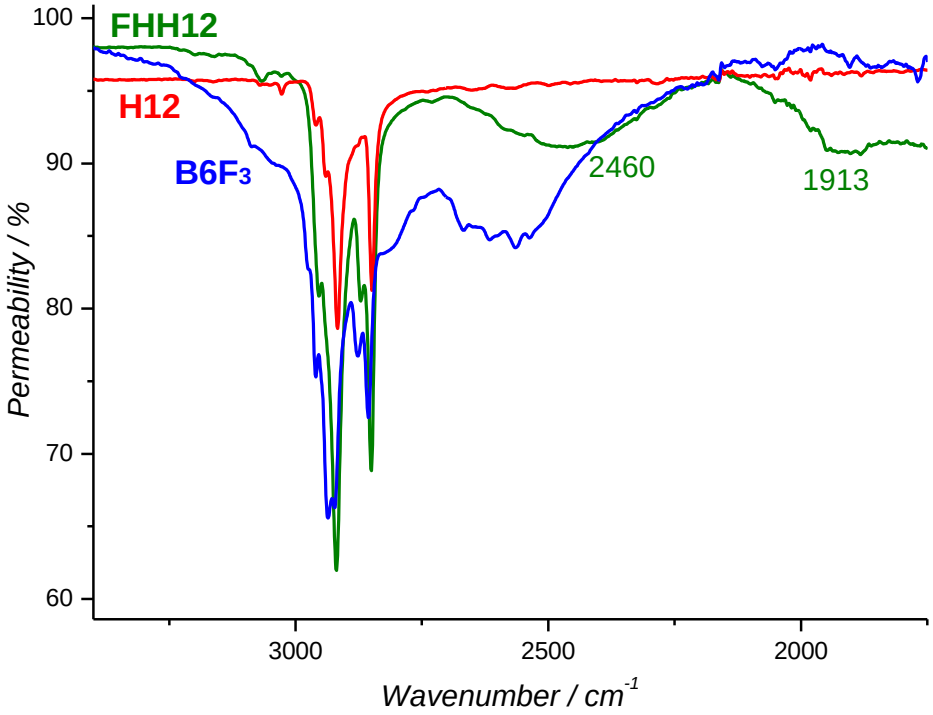

Figure S14b. FTIR spectra of the supramolecule F**HH12** (green) and its complementary components **B6F3** (blue), **AH12** (red) in the crystalline state at room temperature enlarged area between 1750 $cm^{-1}$and 3500 cm^{-1}

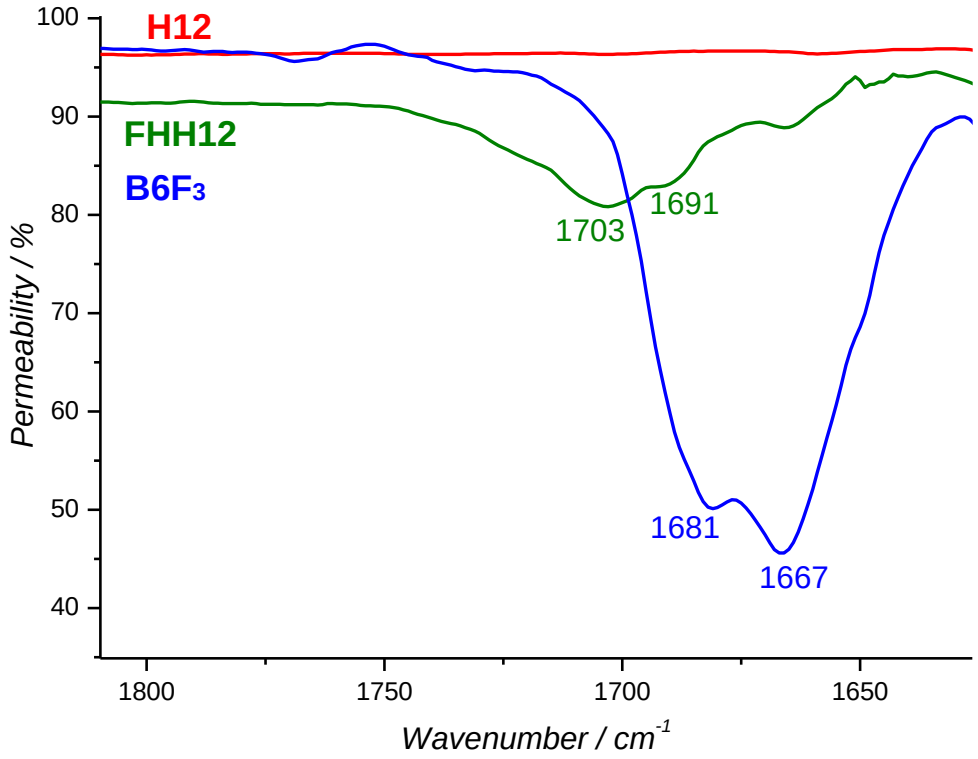

Figure S14c. FTIR spectra of the supramolecule F**HH12** (green) and its complementary components **B6F$_3$** (blue), **AH12** (red) in the crystalline state at room temperature enlarged area between 1625 cm^{-1}and 1800 cm^{-1}

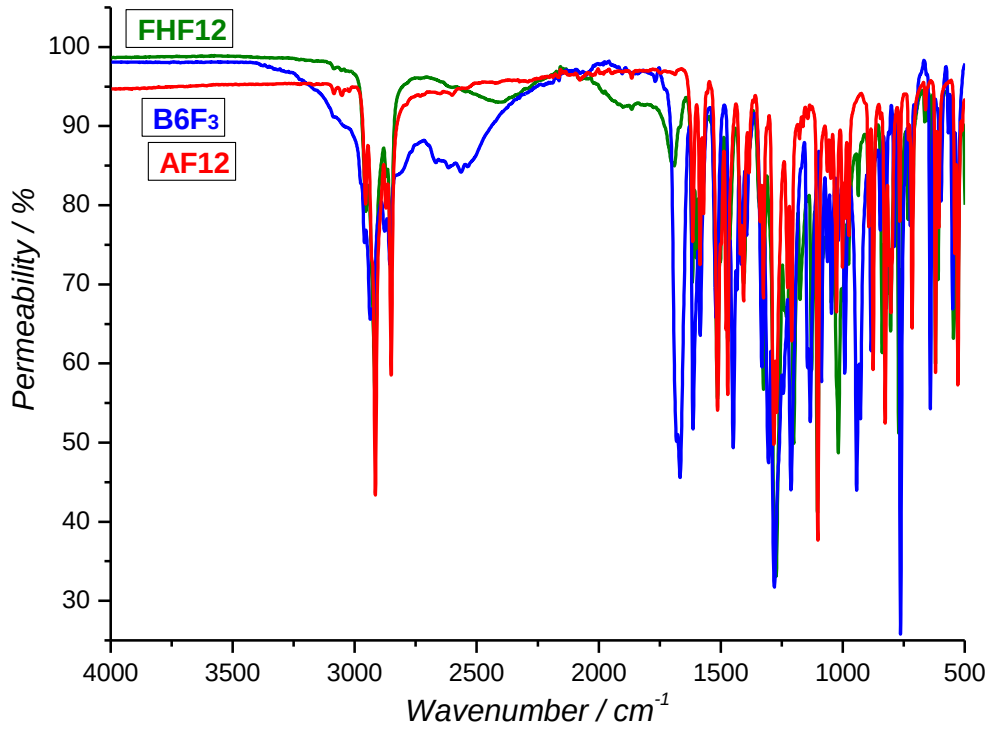

Figure S15a. FTIR spectra of the supramolecule **FHF12** (green) and its complementary components **B6F$_3$** (blue), **AF12** (red) in the crystalline state (KBr) at room temperature.

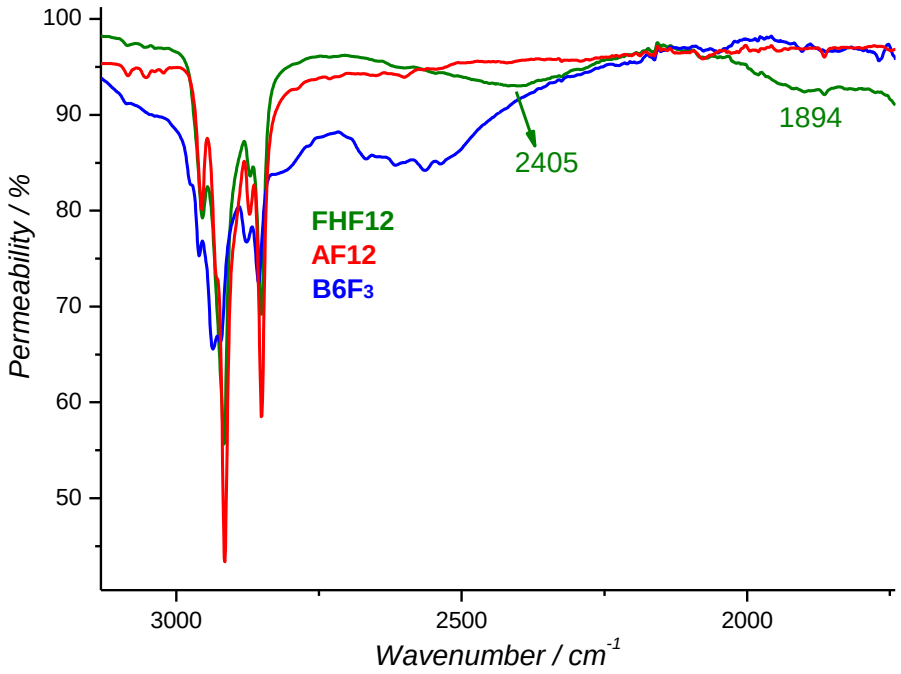

Figure S15b. FTIR spectra of the supramolecule F**HF12** (green) and its complementary components **B6F$_3$** (blue), **AF12** (red) in the crystalline state at room temperature enlarged area between 1750 cm^{-1}and 3000 cm^{-1}

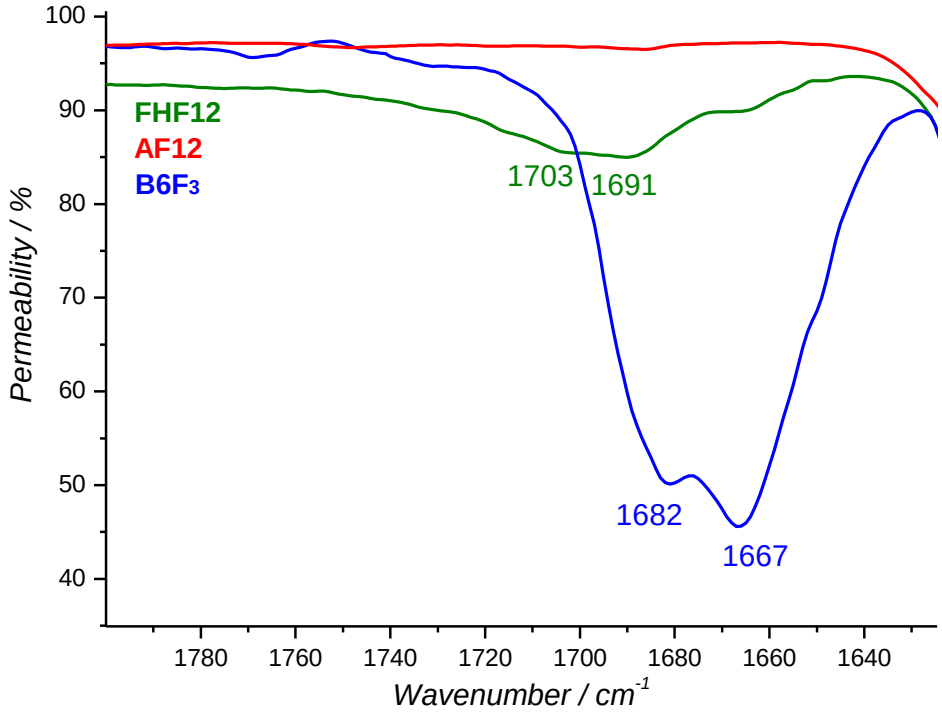

Figure S15c. FTIR spectra of the supramolecule F**HF12** (green) and its complementary components **B6F$_3$** (blue), **AF12** (red) in the crystalline state at room temperature enlarged area between 1630 cm^{-1}and 1790 cm^{-1}

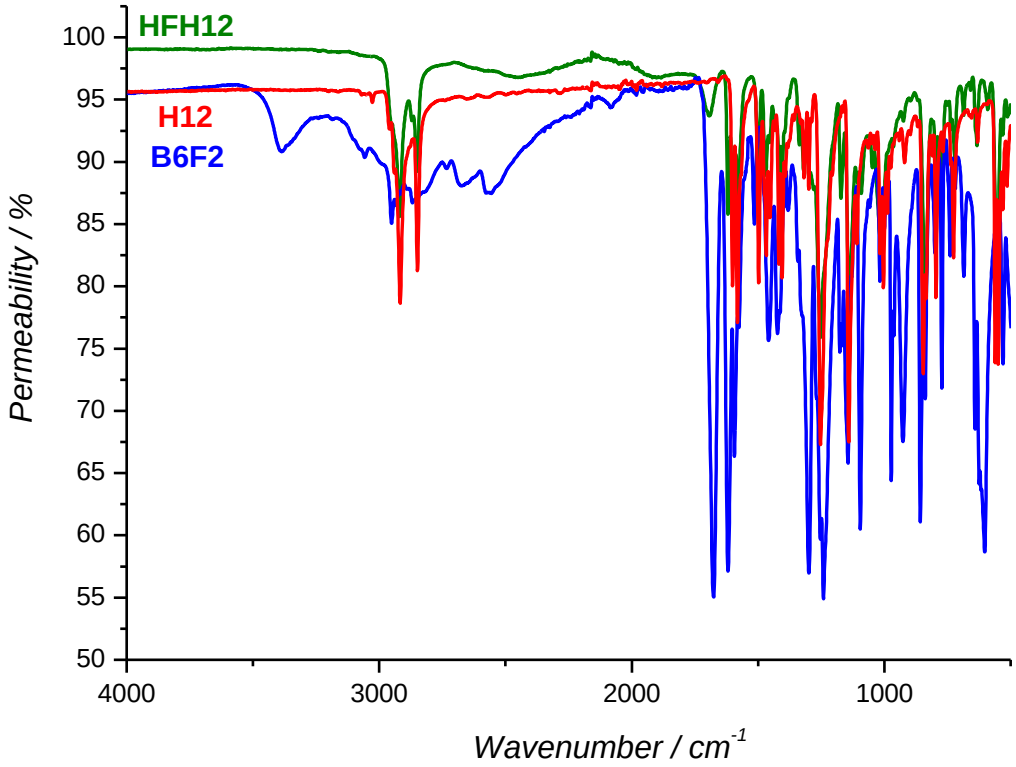

Figure S16a. FTIR spectra of the supramolecule **HFH12** (green) and its complementary components **B6F$_2$** (blue), **AH12** (red) in the crystalline state (KBr) at room temperature.

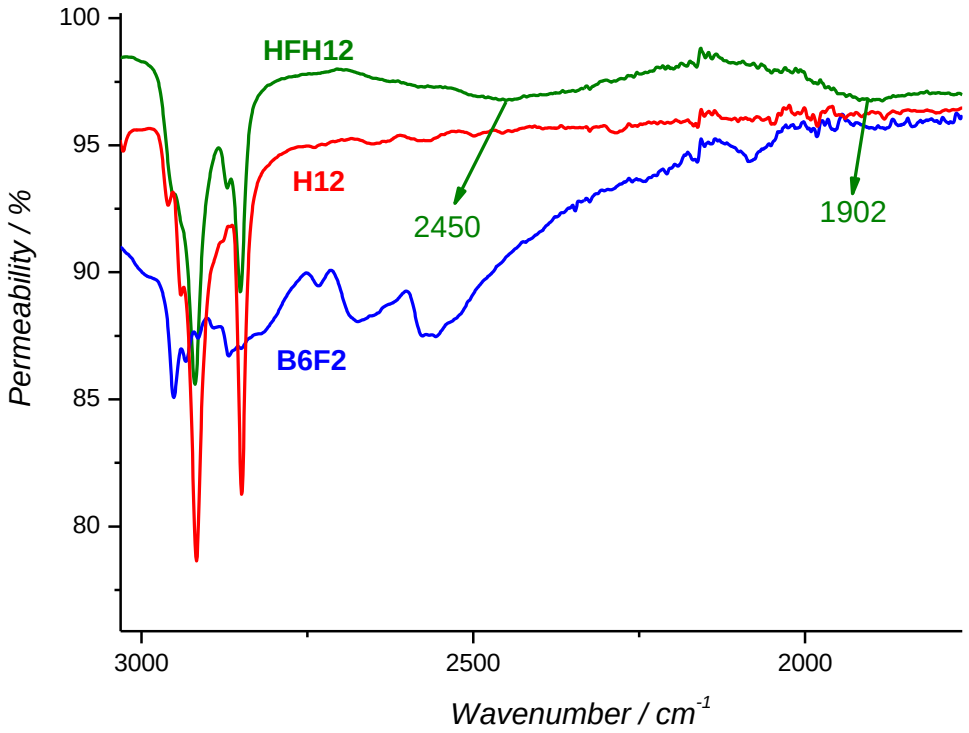

Figure S16b. FTIR spectra of the supramolecule HFH**12** (green) and its complementary components **B6F$_2$** (blue), **AH12** (red) in the crystalline state at room temperature enlarged area between 1750 cm^{-1}and 3000 cm^{-1}

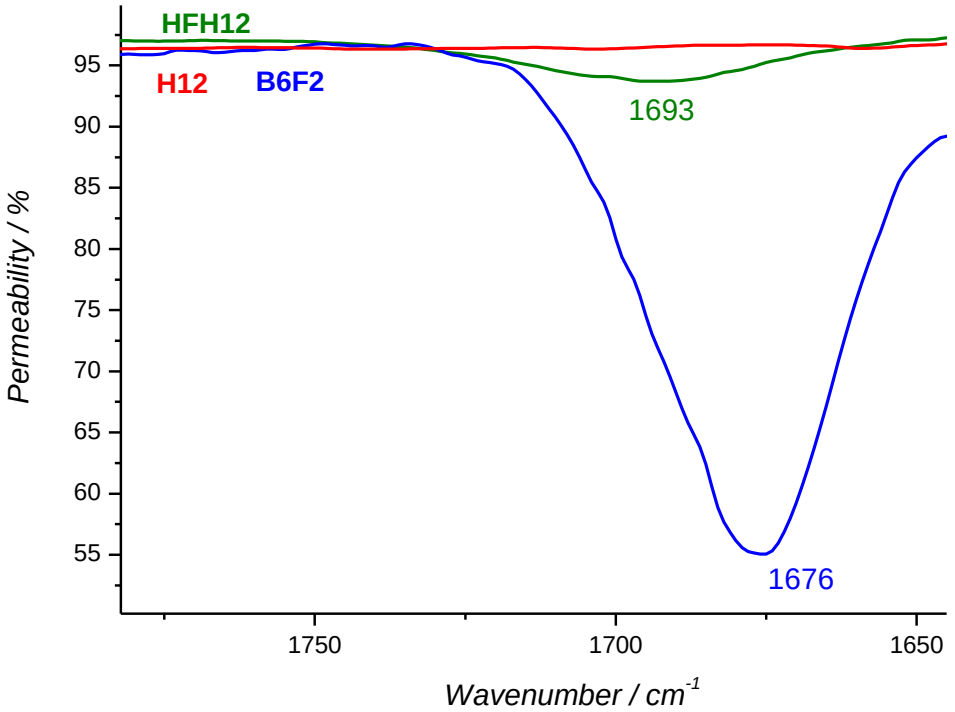

Figure S16c. FTIR spectra of the supramolecule HFH**12** (green) and its complementary components **B6F$_2$** (blue), **AH12** (red) in the crystalline state at room temperature enlarged area between 1650 cm^{-1}and 1775 cm^{-1}

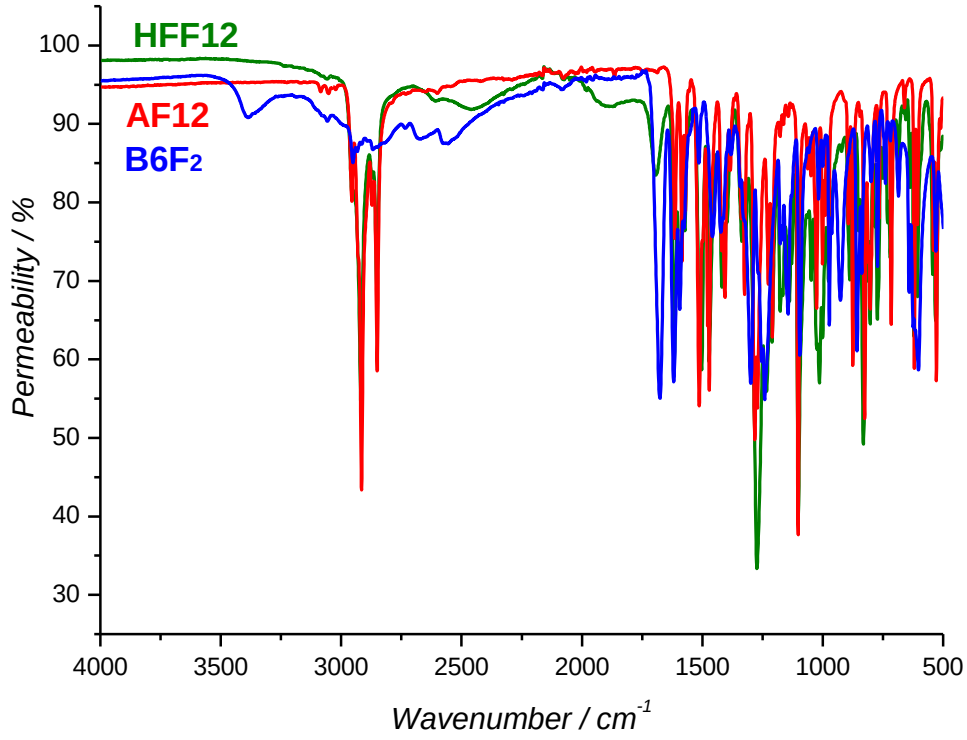

Figure S17a. FTIR spectra of the supramolecule **HFF12** (green) and its complementary components **B6F$_2$** (blue), **AF12** (red) in the crystalline state (KBr) at room temperature.

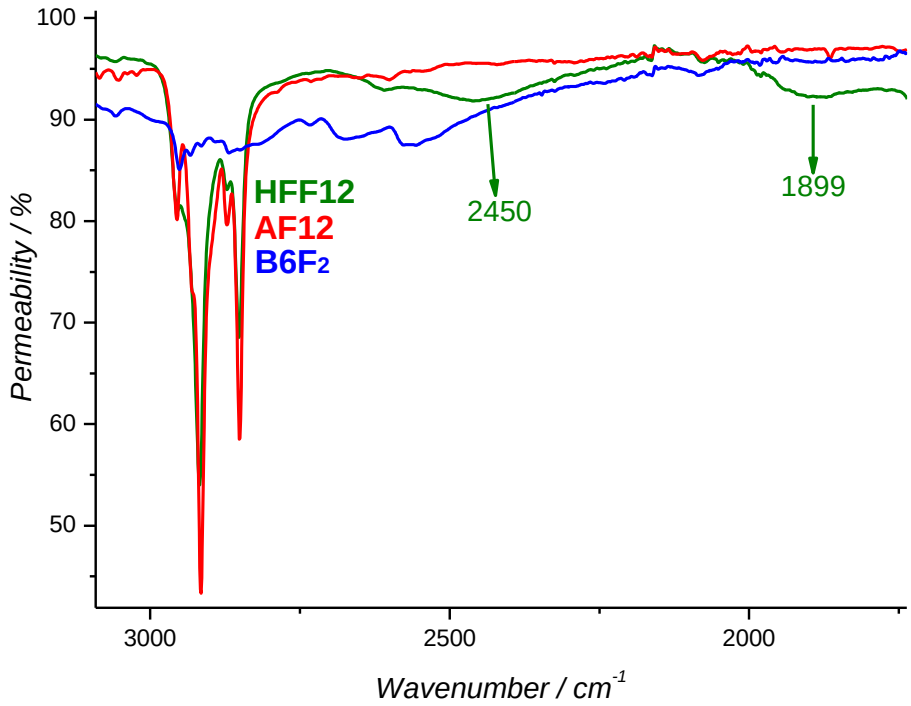

Figure S17b. FTIR spectra of the supramolecule HFF**12** (green) and its complementary components **B6F$_2$** (blue), **AF12** (red) in the crystalline state at room temperature enlarged area between 1750 cm^{-1}and 3000 cm^{-1}

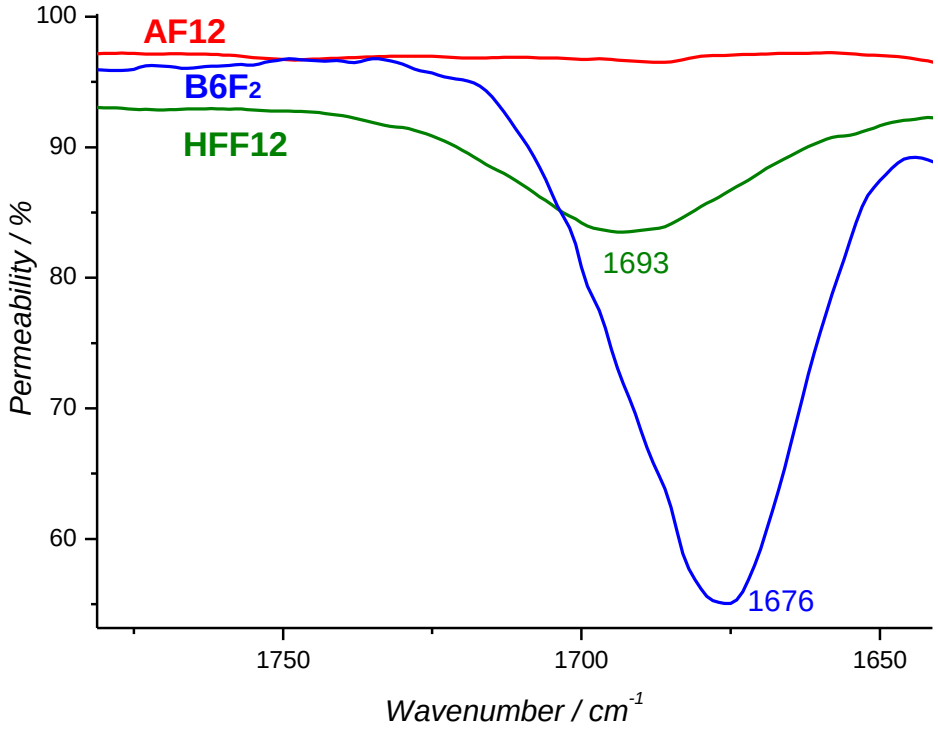

Figure S17c. FTIR spectra of the supramolecule HFF**12** (green) and its complementary components **B6F$_2$** (blue), **AF12** (red) in the crystalline state at room temperature enlarged area between 1650 cm^{-1}and 1775 cm^{-1}

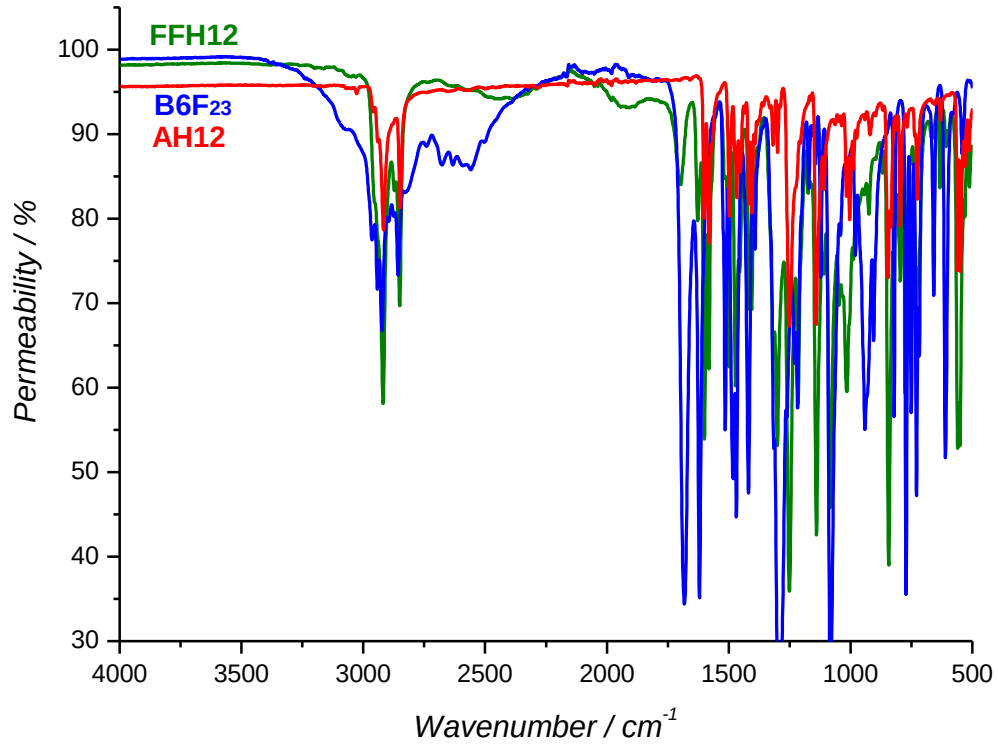

Figure S18a. FTIR spectra of the supramolecule **FFH12** (green) and its complementary components **B6F$_{23}$** (blue), **AH12** (red) in the crystalline state (KBr) at room temperature.

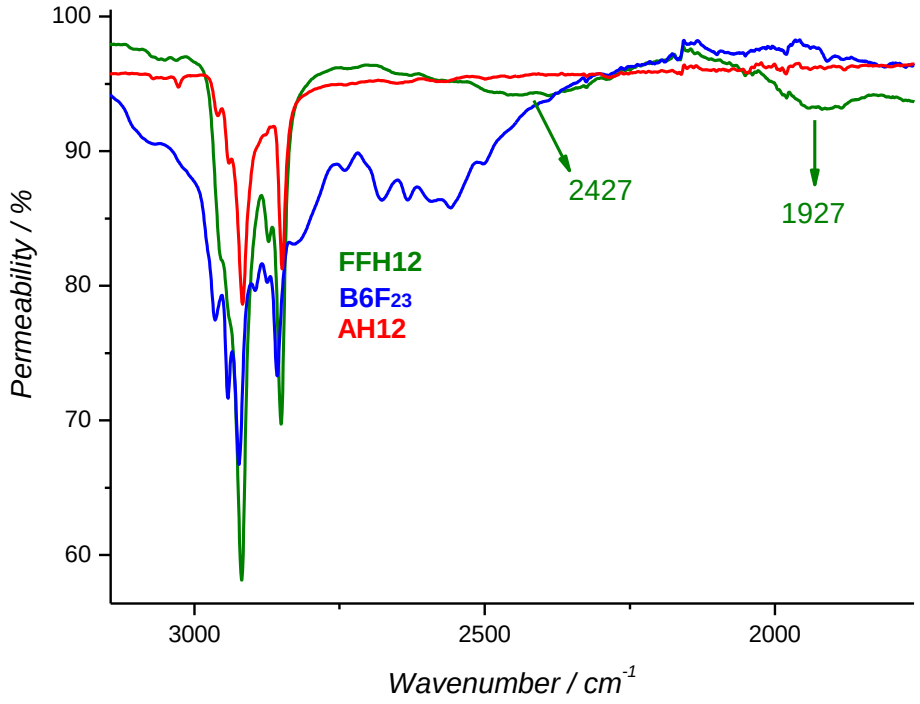

Figure S18b. FTIR spectra of the supramolecule **FFH12** (green) and its complementary components **B6F$_{23}$** (blue), **AH12** (red) in the crystalline state (KBr) at room temperature enlarged area between 1750 cm^{-1}and 3000 cm^{-1}

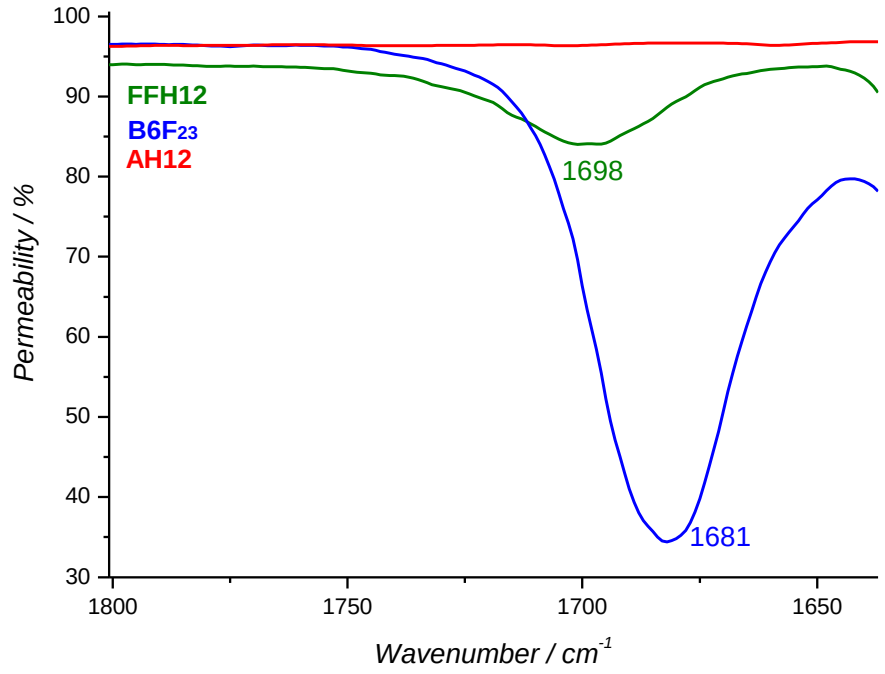

Figure S18c. FTIR spectra of the supramolecule **FFH12** (green) and its complementary components **B6F$_{23}$** (blue), **AH12** (red) in the crystalline state (KBr) at room temperature enlarged area between 1650 cm^{-1}and 1800 cm^{-1}

4. NMR Charts of hydrogen-bonded supramolecules

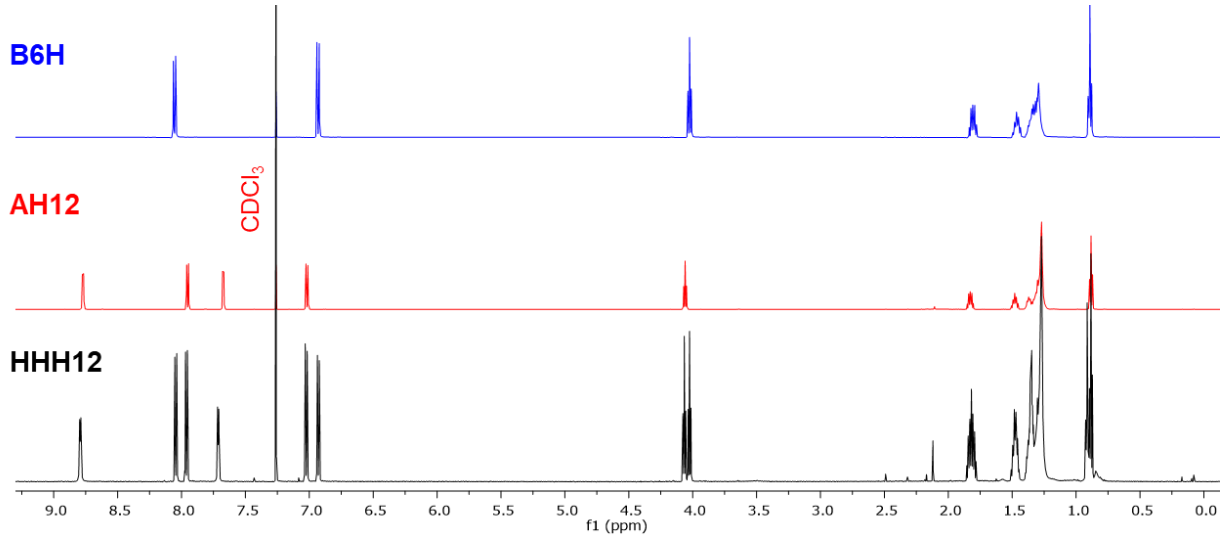

Figure S19. ^{1}HNMR spectra (500 MHz, $CDCl_3$) of the supramolecule **HHH12** (black) and its complementary components the azopyridine derivative **AH12** (red) and the benzoic acid derivative **B6H** (blue).

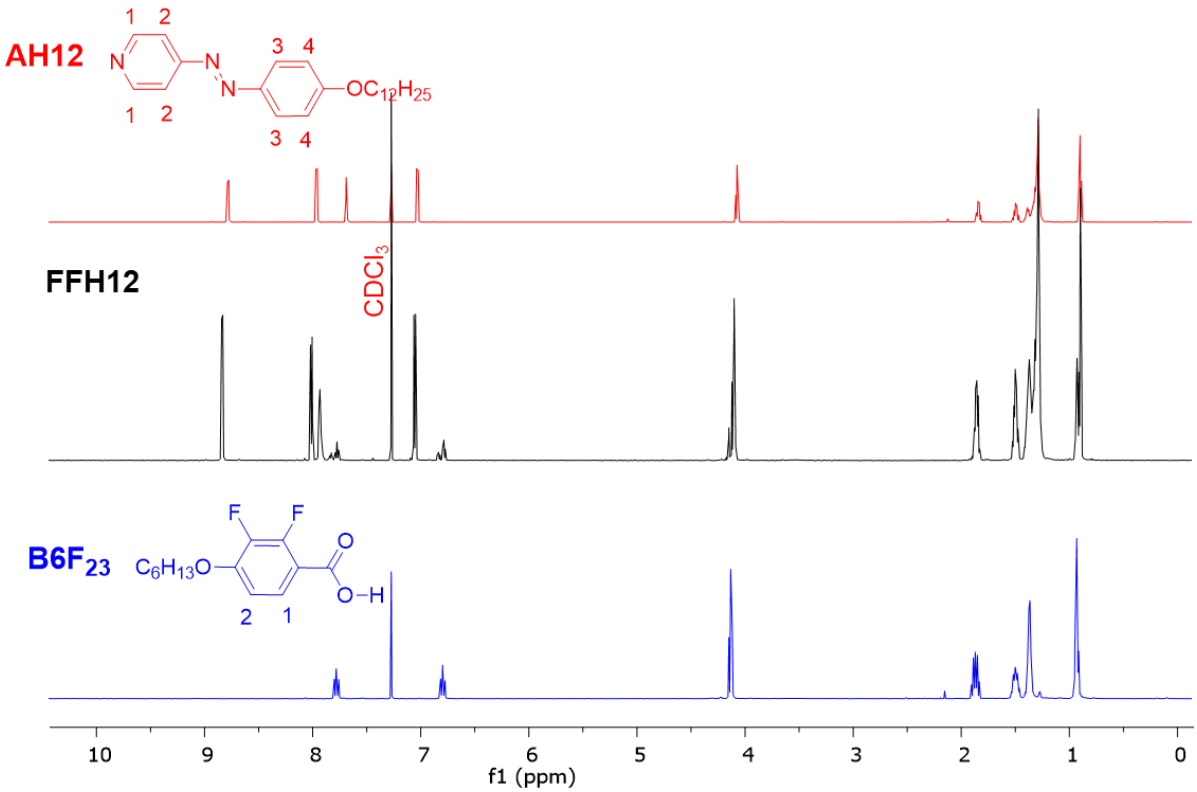

Figure S20. ^{1}HNMR spectra (500 MHz, $CDCl_3$) of the supramolecule **FFH12** (black) and its complementary components the azopyridine derivative **AH12** (red) and the benzoic acid derivative **B6F$_{23}$** (blue).

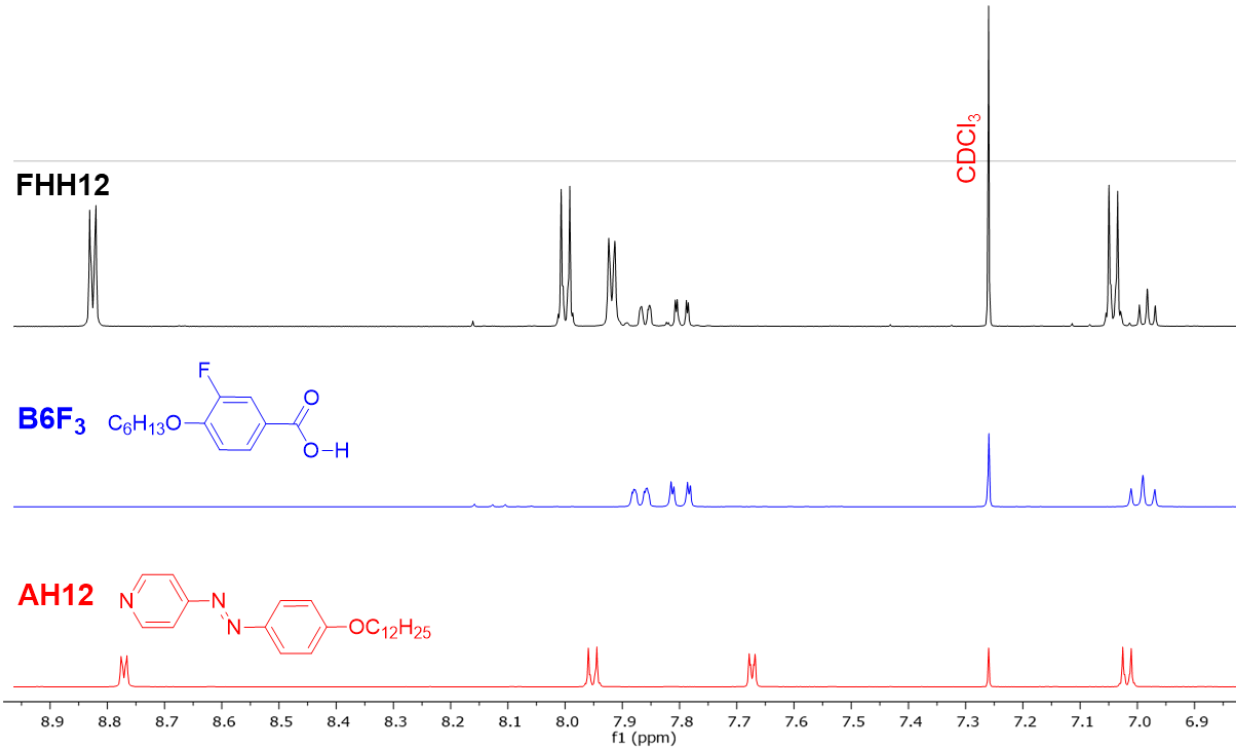

Figure S21a. ^{1}HNMR spectra (500 MHz, $CDCl_3$) in the aromatic region of the supramolecule **FHH12** (black) and its complementary components the azopyridine derivative **AH12** (red) and the benzoic acid derivative **B6F$_3$** (blue).

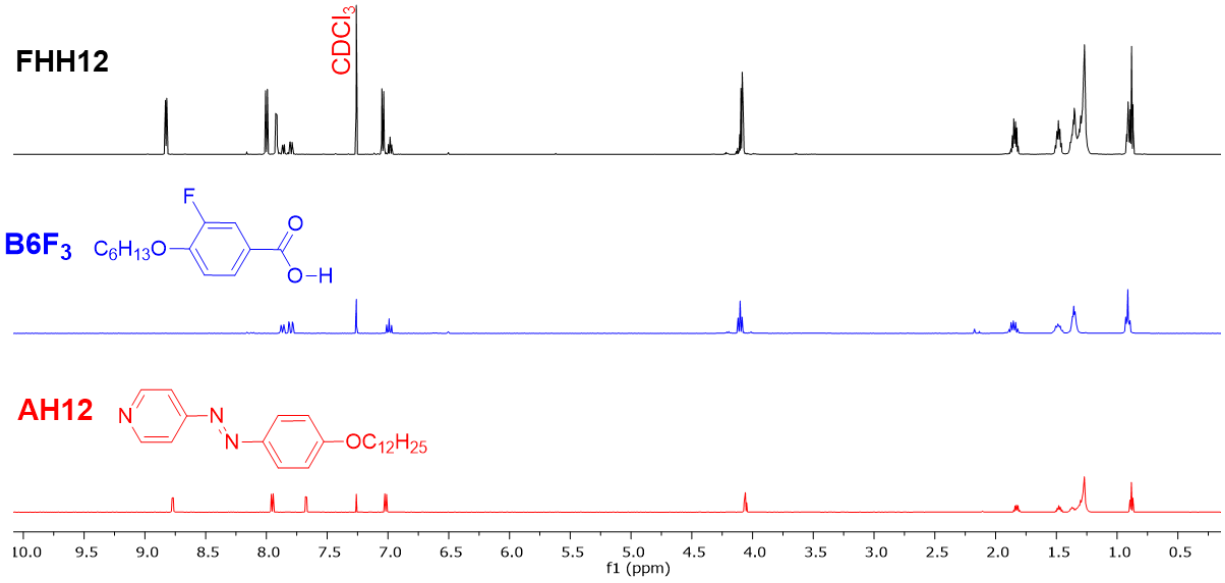

Figure S21b. ^{1}HNMR spectra (500 MHz, $CDCl_3$) of the supramolecule **FHH12** (black) and its complementary components the azopyridine derivative **AH12** (red) and the benzoic acid derivative **B6F$_3$** (blue).

5. Tables of transition temperatures

Table S1. Phase transition temperatures (T/°C) of the azopyridine derivatives **AH*n*** and **AF*n***.[a1,2]

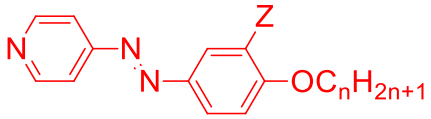

Comp.	Z	Heating (*T*/°C)
AH8	H	Cr 71 Iso
AH10	H	Cr 67 Iso
AH12	H	Cr 73 Iso
AH14	H	Cr 74 Iso
AF8	F	Cr 58 Iso
AF10	F	Cr 57 Iso
AF12	F	Cr 66 Iso
AF14	F	Cr 68 Iso

Notes: [a] Peak temperatures as determined from POM; abbreviations: Cr = crystalline solid; Iso = isotropic liquid.

Table S2. Phase transition temperatures (T/°C) of the benzoic acid derivatives **B6H**, **B6F$_2$**, **B6F$_3$** and **B6F$_{23}$**.[a]

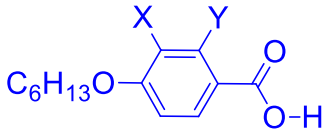

Comp.	X	Y	Heating (*T*/°C)
B6H	H	H	Cr 104 N 134 Iso
B6F$_2$	H	F	Cr 110 N 120 Iso
B6F$_3$	F	H	Cr 108 Iso
B6F$_{23}$	F	F	Cr 108 Iso

Notes: [a] Peak temperatures as determined from POM; abbreviations: Cr = crystalline solid; N= nematic phase; Iso = isotropic liquid.

Table S3. DSC data scanned at the rate of 10 °C/min for different series of **HHH*n*** HBLCs[a].

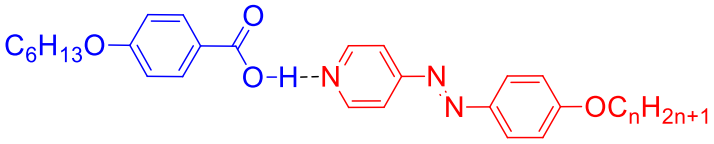

Complex	Phase sequence (T/°C [ΔH(J/g)])[a]
HHH8	**H**: Cr 106 [56.2] SmA 124 [4.1] N 134 [7.0] Iso
	C: Iso 131 [-6.8] N 121 [-4.4] SmA 97 [-54.2] Cr
HHH10	**H**: Cr1 82 [18.9] Cr2 95 [48.0] SmA 128 [20.7] N 131 [20.7][c] Iso
	C: Iso 128 [-19.5] N 125 [-19.5][c] SmA 84 [-44.5] Cr
HHH12	**H**: Cr1 87 [30.3] Cr2 94 [38.5] SmC 110 [< 0.1][b] SmA 131 [23.4] Iso
	C: Iso 127 [-22.3] SmA 108 [< 0.1][b] SmC 84 [-41.0] Cr
HHH14	**H**: Cr 90 [40.8] SmC 116 [< 0.1][b] SmA 131 [12.8] Iso
	C: Iso 129 [-12.5] SmA 114 [< 0.1][b] SmC 83 [-17.2] Cr

N = nematic phase, SmA = Smectic A, SmC = Smectic C. [b]Enthalpy value is undetectable by DSC, [c]cannot be separated.

Table S4. DSC data scanned at the rate of 10 °C/min for different series of **HHF*n*** HBLCs[a].

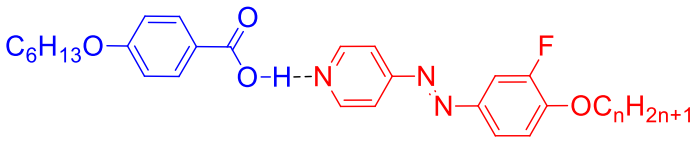

Complex	Phase sequence (T/°C [ΔH(J/g)])[a]
HHF8	**H**: Cr 101 [57.9] N 118 [5.1] Iso
	C: Iso 115 [-5.6] N 84 [-53.3] Cr
HHF10	**H**: Cr 87 [55.5] SmC 95[1.1] N 113 [3.7] Iso
	C: Iso 110 [-4.8] N 92 [-1.5] SmC 70 [-55.5] Cr
HHF12	**H:** Cr 96 [49.3] SmC 112 [< 0.1][c] N 114 [9.9] Iso
	C: Iso 110 [-11.7] N 102 [< 0.1][b] SmC 73 [-50.9] Cr
HHF14	**H:** Cr 95 [56.3] SmC 111 [14.4] Iso
	C: Iso 108 [-13.8] SmC 74 [-64.1] Cr

For abbreviations see Table S1. [b]Enthalpy value is undetectable by DSC, [c]cannot be separated.

Table S5. DSC data scanned at the rate of 10 °C/min for different series of **FHH*n*** HBLCs[a].

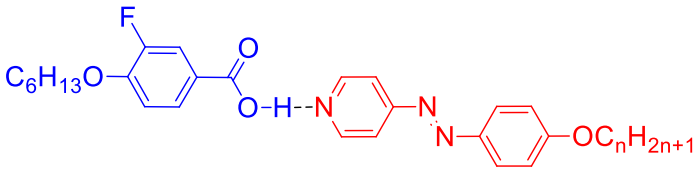

Complex	Phase sequence (T/°C [ΔH(J/g)])[a]
FHH8	**H:** Cr 89 [33.7] SmA 126 [15.6] Iso
	C: Iso 120 [-13.8] SmA 90 [< 0.01][b] SmC 79 [-32.5] Cr
FHH10	**H:** Cr 85 [29.3] SmC 100 [< 0.01][b] SmA 125 [15.8] Iso
	C: Iso 119 [-13.5] SmA 98 [< 0.01][b] SmC 75 [-27.7] Cr
FHH12	**H:** Cr 80 [28.8] SmC 112 [< 0.1][b] SmA 124 [19.7] Iso
	C: Iso 121 [-19.1] SmA 110 [< 0.1][b] SmC 76 [-27.6] Cr
FHH14	**H:** Cr 62 [24.4] SmC 114 [< 0.01][b] SmA 126 [5.9] Iso
	C: Iso 121 [-4.4] SmA 112 [< 0.01][b] SmC 49 [-22.7] Cr

For abbreviations see Table S1. [b]Enthalpy value is undetectable by DSC.

Table S6. DSC data scanned at the rate of 10 °C/min for different series of **FHF*n*** HBLCs[a].

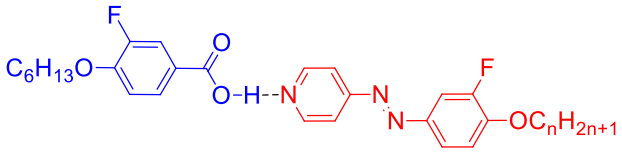

Complex	Phase sequence (T/°C [ΔH(J/g)])[a]
FHF8	**H:** Cr 82 [53.3] SmC 90 [< 0.1][b] SmA 100 [6.5][c] N 105 [6.5][c] Iso
	C: Iso 99 [-8.6][c] N 88 [-8.6][c] SmA 84 [< 0.1] SmC 67 [-52.8] Cr
FHF10	**H:** Cr 89 [72.7] SmC 98 [< 0.01][b] SmA 107 [6.9] Iso
	C: Iso 100 [-9.6][c] SmA 93 [-9.6][c] SmC 77 [-71.6] Cr
FHF12	**H:** Cr 87 [54.8] SmC 90 [9.6][c] SmA 110 [9.6] Iso
	C: Iso 102 [-10.6][c] SmA 100 [-10.6][c] SmC 72 [-53.9] Cr
FHF14	**H:** Cr 94 [66.3] SmC 100 [11.5][c] SmA 111 [11.5][c] Iso
	C: Iso 105 [-10.1] SmA 98 [-9.6][c] SmC 79 [-67.5] Cr

For abbreviations see Table S1. [b]Enthalpy value is undetectable by DSC, [c]cannot be separated.

Table S7. DSC data scanned at the rate of 10 °C/min for different series of **HFH*n*** HBLCs[a].

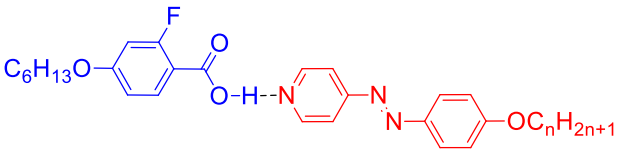

Complex	Phase sequence (T/°C [ΔH(J/g)])[a]
HFH8	**H:** Cr 96 [62.7] N122 [9.9] Iso
	C: Iso 118 [-5.5] N 52 [-53.5] Cr
HFH10	**H:** Cr 85 [50.3] X 105 [1.9] N 119 [6.7] Iso
	C: Iso 115 [-6.9] N 102 [-2.7] X 67 [-26.7] Cr
HFH12	**H:** Cr 82 [64.7] X 112[18.2][c] N 118 [18.2][c] Iso
	C: Iso 116 [-17.9][c] N 110 [-17.9][c] X 74 [-29.5] Cr
HFH14	**H:** Cr 83 [62.3] X 114 [18.2][c] N 118 [18.9][c] Iso
	C: Iso 115 [-17.8][c] N 112 [-17.8][c] X 68 [-50.8] Cr

X = Unknown LC phase; for other abbreviations see Table S1. [c]Enthalpy value cannot be separated.

Table S8. DSC data scanned at the rate of 10 °C/min for different series of **HFF*n*** HBLCs[a].

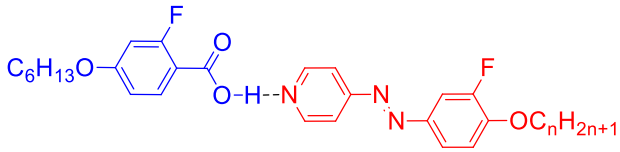

Complex	Phase sequence (T/°C [ΔH(J/g)])[a]
HFF8	**H:** Cr 87 [38.8] N 105 [3.1] Iso
	C: Iso 103 [-2.8] N 70 [-19.6] Cr
HFF10	**H:** Cr 85 [39.8] N 100 [4.7] Iso
	C: Iso 99 [-4.5] N 52 [-49.2] Cr
HFF12	**H:** Cr 89 [74.0] N 104 [4.7] Iso
	C: Iso 101 [-5.8] N 72 [-0.4] Nx 51 [-48.2] Cr
HFF14	**H:** Cr 94 [66.3] SmC 100 [11.5][c] SmA 111 [11.5][c] Iso
	C: Iso 105 [-10.1] SmA 98 [-9.6][c] SmC 79 [-67.5] Cr

Nx = Unknown nematic phase; for abbreviations see Table S1. [b]Enthalpy value cannot be separated.

Table S9. DSC data scanned at the rate of 10 °C/min for different series of **FFH*n*** HBLCs[a].

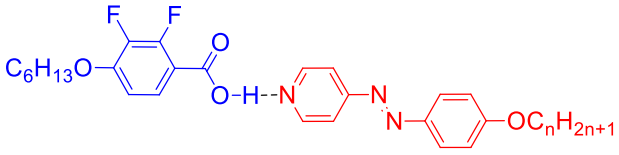

Complex	Phase sequence (T/°C [ΔH(J/g)])[a]
FFH8	**H:** Cr 106 [47.2] SmC 115 [0.6] SmA 123 [13.7][c] N 130 [13.7][c] Iso
	C: Iso 128 [-14.5][c] N 122 [-14.5][c] SmA 113 [-0.7] SmC 100 [-46.9] Cr
FFH10	**H:** Cr 104 [45.4] SmC 122 [18.5][c] SmA 128 [18.5] Iso
	C: Iso 125 [-18.1] SmA 120 [-18.1][c] SmC 96 [-44.8] Cr
FFH12	**H:** Cr 98 [44.4][b] SmC 129 [21.2] Iso
	C: Iso 126 [-22.1] SmC 87 [-43.0] Cr
FFH14	**H:** Cr 97 [46.7] SmC 130 [22.1] Iso
	C: Iso 126 [-21.3] SmC 83 [-43.5] Cr

For abbreviations see Table S1. [b]Enthalpy value is undetectable by DSC, [c]cannot be separated.

Table S10. DSC data scanned at the rate of 10 °C/min for different series of **FFF*n*** HBLCs[a].

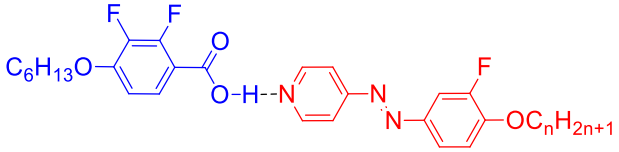

Complex	Phase sequence (T/°C [ΔH(J/g)])[a]
FFF8	**H:** Cr 93 [55.4] SmC 104 [16.2][c] N 114 [16.2][c] Iso
	C: Iso 111 [-14.7][c] N 100 [-14.7][c] SmC 83 [-51.5] Cr
FFF10	**H:** Cr 89 [47.8] SmC 107 [12.3][c] N 114 [12.3][c] Iso
	C: Iso 112 [-10.9][c] N 104 [-10.9][c] SmC 80 [-38.7] Cr
FFF12	**H:** Cr 91 [60.8] SmC 116 [18.4] Iso
	C: Iso 111 [-16.6] SmC 79 [-55.9] Cr
FFF14	**H:** Cr 95 [56.2] SmC 119 [16.9] Iso
	C: Iso 113 [-17.6] SmC 81 [-48.0] Cr

For abbreviations see Table S1. [b]Enthalpy value cannot be separated.

6. Additional DSC Plots

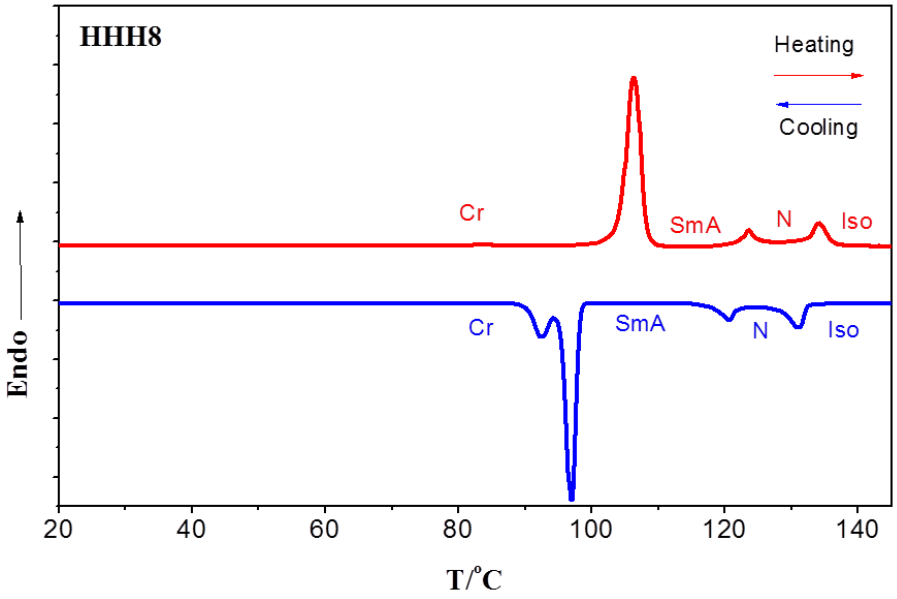

Figure S22. DSC Heating and cooling cycles of the HBLC **HHH8** at a scanning rate of 10 °C/min.

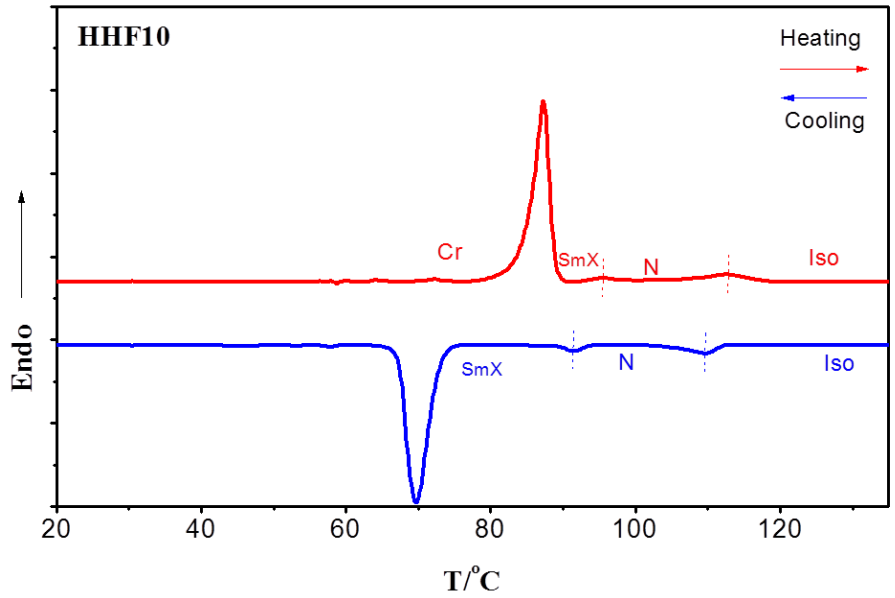

Figure S23. DSC Heating and cooling cycles of the HBLC **HHF10** at a scanning rate of 10 °C/min.

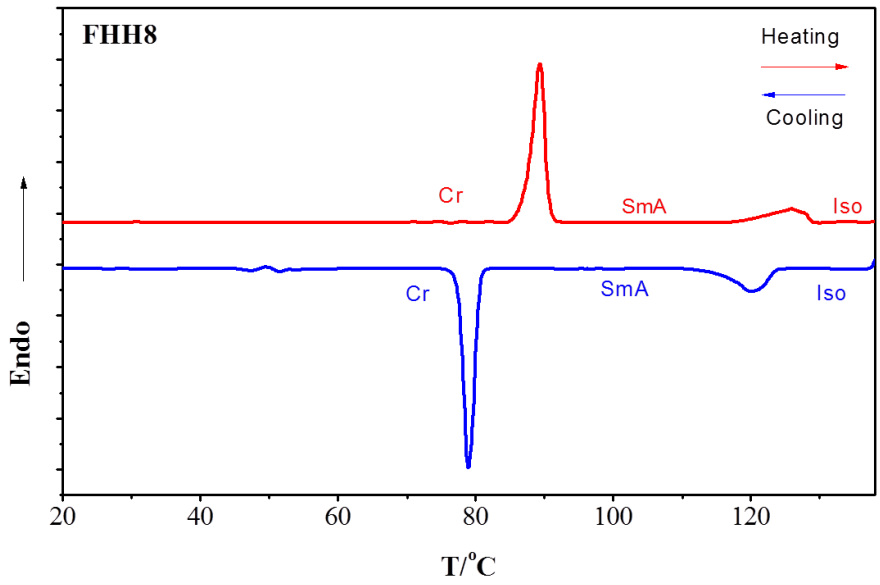

Figure S24. DSC Heating and cooling cycles of the HBLC **FHH8** at a scanning rate of 10 °C/min.

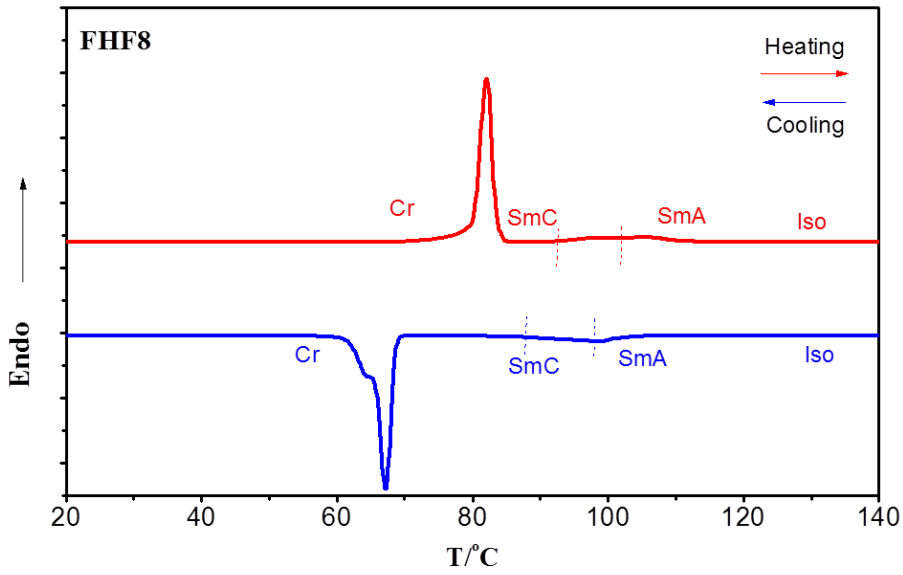

Figure S25. DSC Heating and cooling cycles of the HBLC **FHF8** at a scanning rate of 10 °C/min.

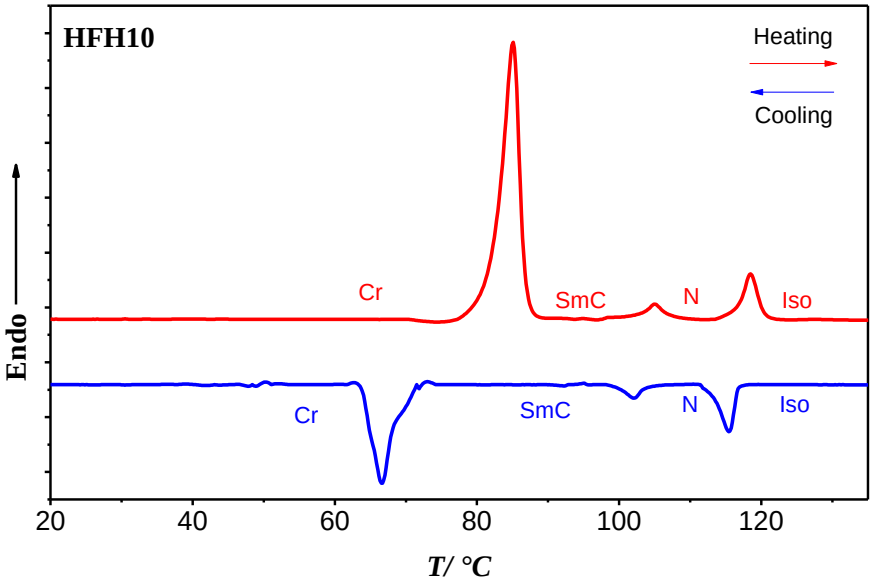

Figure S26. DSC Heating and cooling cycles of the HBLC **HFH10** at a scanning rate of 10 °C/min.

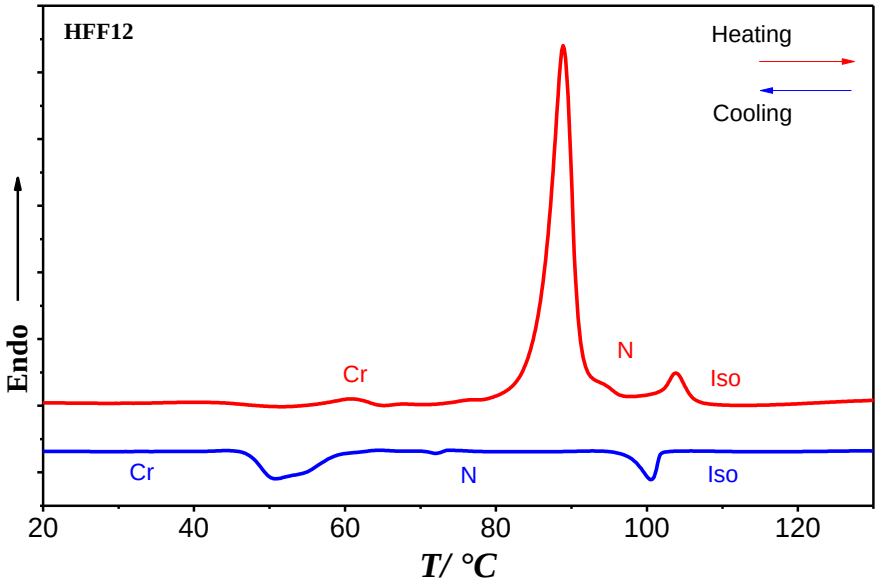

Figure S27. DSC Heating and cooling cycles of the HBLC **HFF12** at a scanning rate of 10 °C/min.

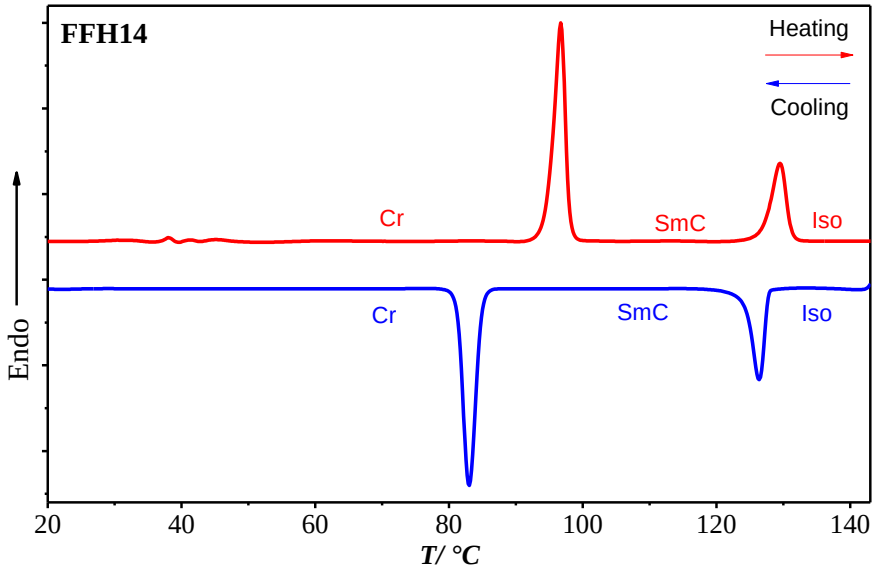

Figure S28. DSC Heating and cooling cycles of the HBLC **FFH14** at a scanning rate of 10 °C/min.

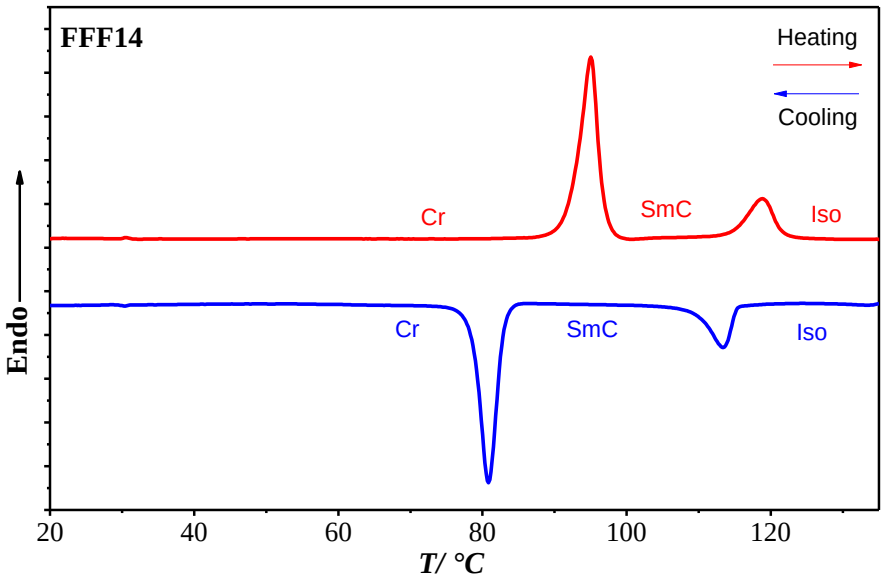

Figure S29. DSC Heating and cooling cycles of the HBLC **FFF14** at a scanning rate of 10 °C/min.

7. Additional XRD data

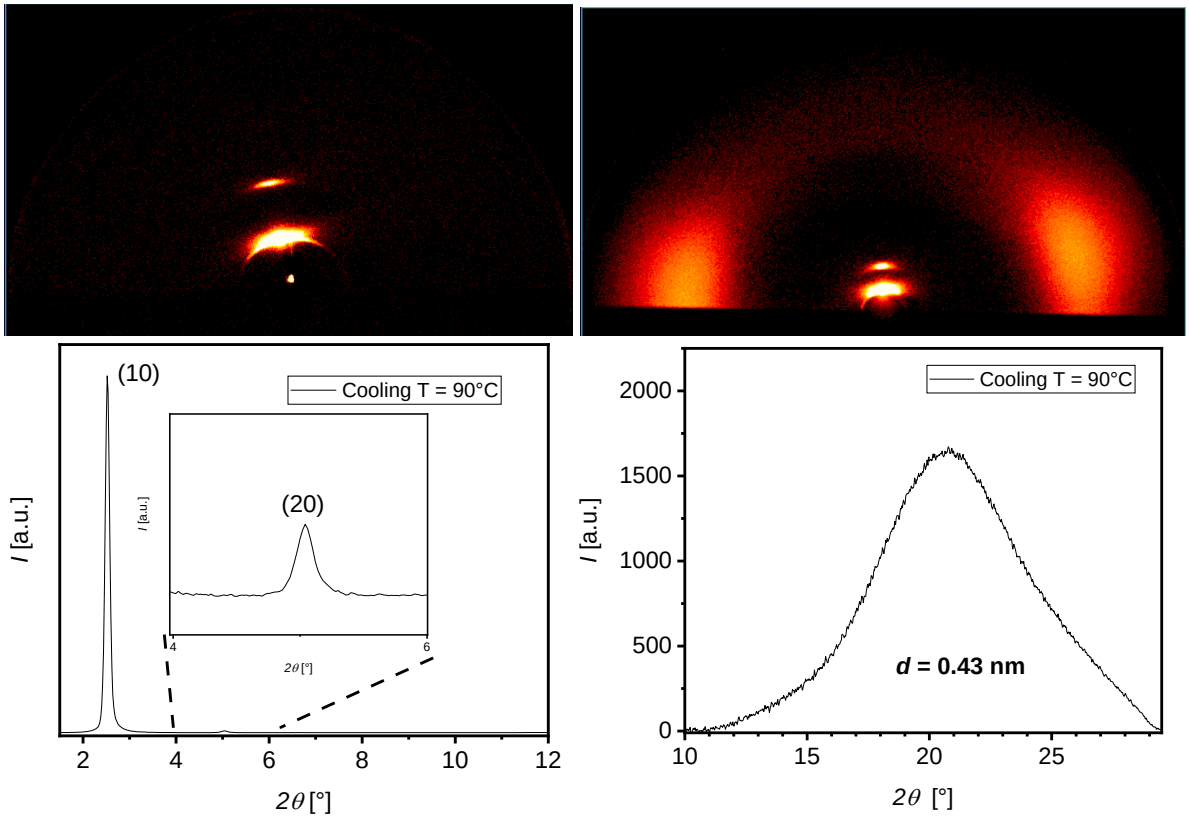

Figure S30. XRD investigations of **FHH8** on cooling in the SmC phase at T = 90 °C. Right column in the small-angle region (SAXS) and left column in the WAXS region.

Table S11. XRD data of the supramolecule **FHH8** at 90 °C.

2θ [°]	**d_{obs} [nm]**	**hkl**
2.270	1.750	10
2.694	0.878	20
20.791	0.427	

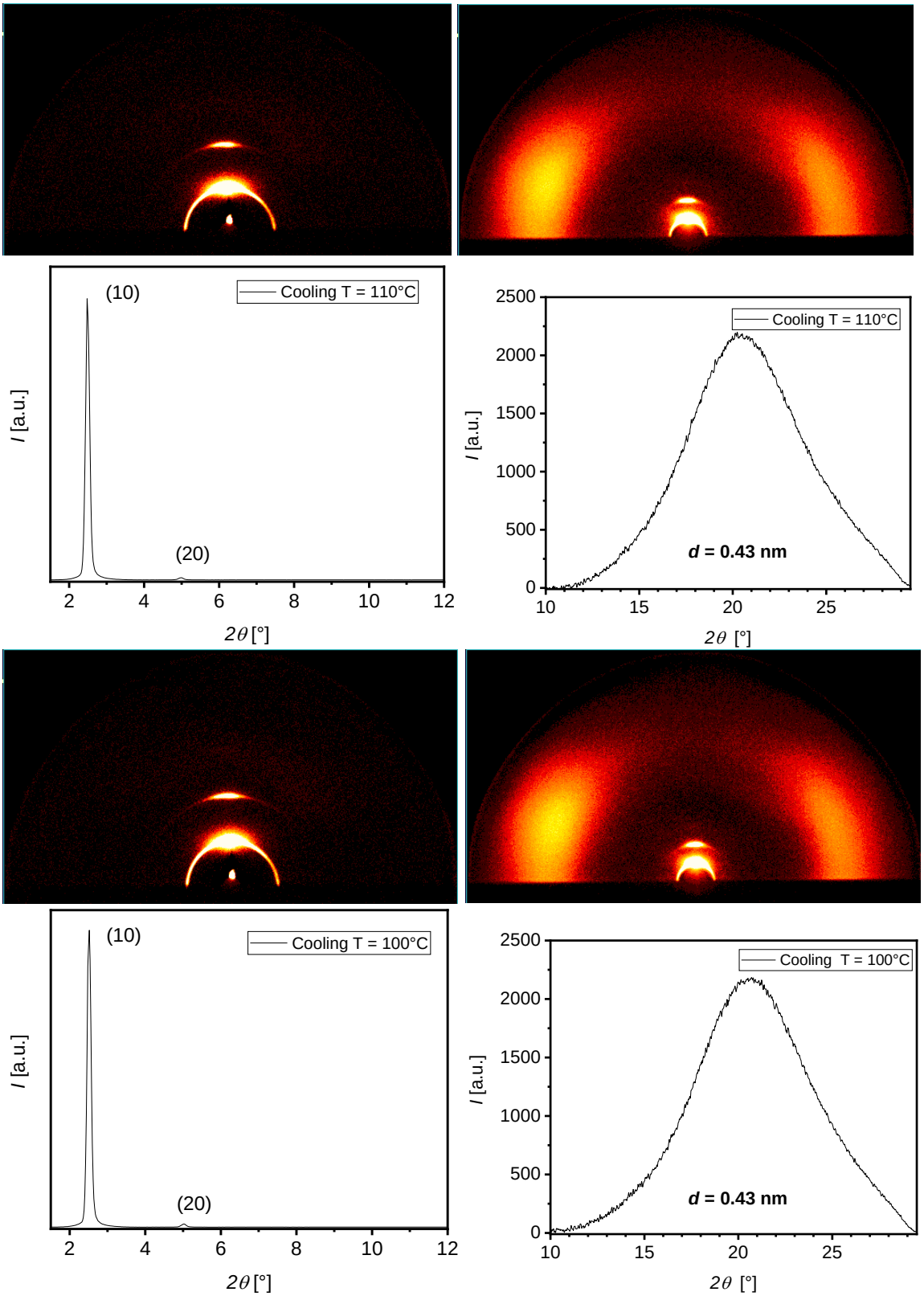

Figure S31. XRD investigations of **FFH12** on cooling in the SmC phase at T = 110 °C and 100 °C. Right column in the small-angle region (SAXS) and left column in the WAXS region.

Table S12. XRD data of the supramolecule **FFH12** at 110 °C.

2θ [°]	d_{obs} [nm]	hkl
2.493	3.544	10
4.982	1.774	20
20.597	0.431	

Table S13. XRD data of the supramolecule **FFH12** at 100 °C.

2θ [°]	d_{obs} [nm]	hkl
2.514	3.514	10
5.018	1.761	20
20.743	0.428	

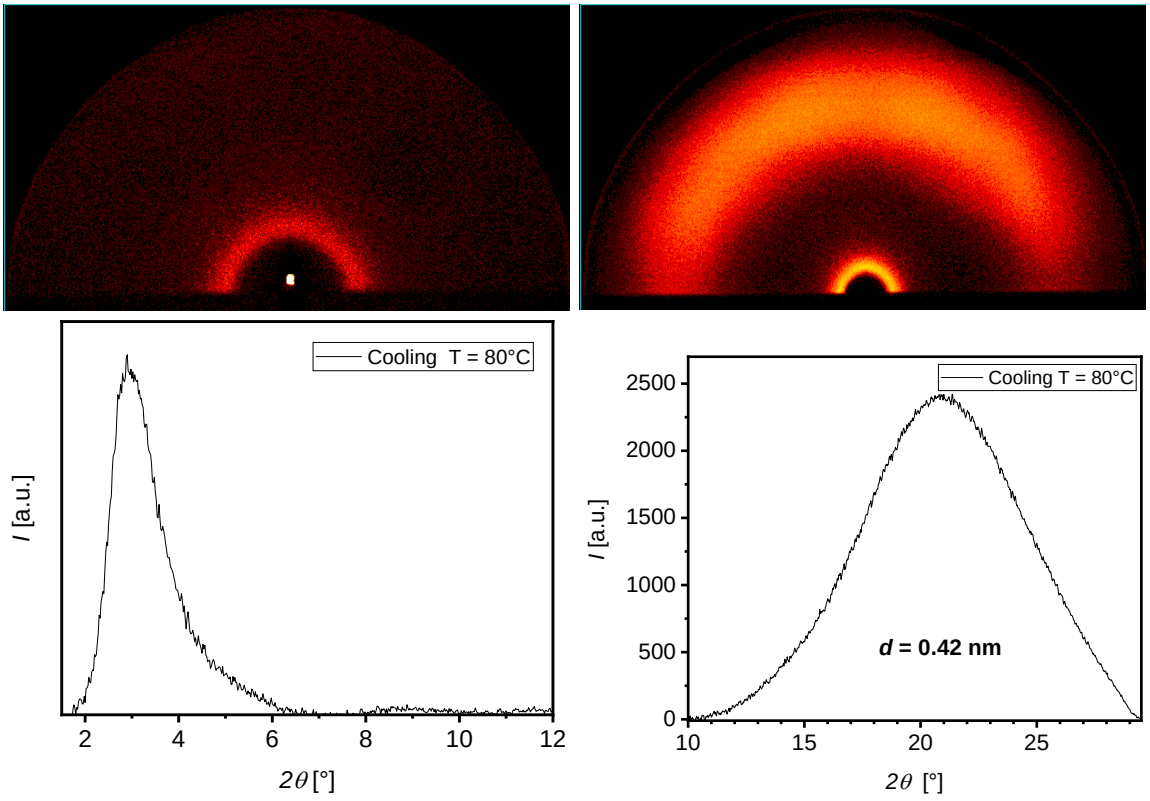

Figure S32. XRD investigations of **HFF8** on cooling in the nematic phase at T = 80 °C. Right column in the small-angle region (SAXS) and left column in the WAXS region.

8. References

1 M. Alaasar, J. C. Schmidt, A. F. Darweesh and C. Tschierske, *J. Mol. Liq.*, 2020, **310**, 113252.

2 M. Alaasar, S. Poppe, Q. Dong, F. Liu and C. Tschierske, *Chem. Commun.*, 2016, **52**, 13869–13872.